

The public reporting burden for this collection of information is estimated to average 1 hour per response, including the time for reviewing instructions, searching existing data sources, gathering and maintaining the data needed, and completing and reviewing the collection of information. Send comments regarding this burden estimate or any other aspect of this collection of information, including suggestions for reducing this burden, to Washington Headquarters Services, Directorate for Information Operations and Reports, 1215 Jefferson Davis Highway, Suite 1204, Arlington VA, 22202-4302. Respondents should be aware that notwithstanding any other provision of law, no person shall be subject to any penalty for failing to comply with a collection of information if it does not display a currently valid OMB control number.  
PLEASE DO NOT RETURN YOUR FORM TO THE ABOVE ADDRESS.

1. REPORT DATE (DD-MM-YYYY) 04-11-2022	2. REPORT TYPE Final Report	3. DATES COVERED (From - To) 8-Dec-2014 - 30-Jun-2022
---	--------------------------------	--

4. TITLE AND SUBTITLE Final Report: Extended-wavelength hot-carrier photodetectors from GaAs, Si to InAs/GaSb type-II structures (d. Research Area 4.3 Electronic Sensing ARO)	5a. CONTRACT NUMBER W911NF-15-1-0018
	5b. GRANT NUMBER
	5c. PROGRAM ELEMENT NUMBER 611102

6. AUTHORS	5d. PROJECT NUMBER 611104
	5e. TASK NUMBER
	5f. WORK UNIT NUMBER

7. PERFORMING ORGANIZATION NAMES AND ADDRESSES Georgia State University University Plaza P.O. Box 3999 Atlanta, GA 30302 -3999	8. PERFORMING ORGANIZATION REPORT NUMBER
--	--

9. SPONSORING/MONITORING AGENCY NAME(S) AND ADDRESS (ES) U.S. Army Research Office P.O. Box 12211 Research Triangle Park, NC 27709-2211	10. SPONSOR/MONITOR'S ACRONYM(S) ARO
	11. SPONSOR/MONITOR'S REPORT NUMBER(S) 66499-PE-H.46

12. DISTRIBUTION AVAILABILITY STATEMENT Approved for public release; distribution is unlimited.
--

13. SUPPLEMENTARY NOTES The views, opinions and/or findings contained in this report are those of the author(s) and should not be construed as an official Department of the Army position, policy or decision, unless so designated by other documentation.
---

14. ABSTRACT
--------------

15. SUBJECT TERMS
-------------------

16. SECURITY CLASSIFICATION OF:	17. LIMITATION OF ABSTRACT	15. NUMBER OF PAGES	19a. NAME OF RESPONSIBLE PERSON Unil Perera
a. REPORT UU	b. ABSTRACT UU	c. THIS PAGE UU	19b. TELEPHONE NUMBER 404-413-6037

# RPPR Final Report

as of 05-Dec-2022

Agency Code: 21XD

Proposal Number: 66499PEH

Agreement Number: W911NF-15-1-0018

## INVESTIGATOR(S):

**Name:** Unil A G Perera uperera@gs

**Email:** uperera@gsu.edu

**Phone Number:** 4044136037

**Principal:** Y

Organization: **Georgia State University**

Address: University Plaza, Atlanta, GA 303023999

Country: USA

DUNS Number: 073425951

EIN:

**Report Date:** 30-Sep-2022

Date Received: 04-Nov-2022

**Final Report** for Period Beginning 08-Dec-2014 and Ending 30-Jun-2022

**Title:** Extended-wavelength hot-carrier photodetectors from GaAs, Si to InAs/GaSb type-II structures (d. Research Area 4.3 Electronic Sensing ARO)

**Begin Performance Period:** 08-Dec-2014

**End Performance Period:** 30-Jun-2022

**Report Term:** 0-Other

Submitted By: Unil Perera

Email: uperera@gsu.edu

Phone: (404) 413-6037

**Distribution Statement:** 1-Approved for public release; distribution is unlimited.

**STEM Degrees:** 4

**STEM Participants:** 20

**Major Goals:** The proposed aims were to (1) design and (2) develop infrared photodetectors with lower dark current compared to conventional photodetectors with similar wavelength thresholds. In general, both the dark current and the photoresponse threshold are governed by the value of  $\Delta$  (activation energy). Here, we propose to develop detectors where the dark current corresponds to a  $\Delta$ , of a shorter wavelength detector, while the photoresponse threshold corresponds to an energy value  $\Delta'$  (where  $\Delta' < \Delta$ ) giving a longer wavelength threshold.

In order to obtain this phenomenon, a graded injector barrier detector consisting of an absorber sandwiched between a graded and a flat collector barrier was designed. The origin of the effective activation energy ( $\Delta'$ ) in a graded injector barrier detector is also an issue to be understood in order to implement this effect to use this significant novel concept in the area of photodetection. This effective  $\Delta'$  leads to a longer wavelength threshold while the dark current will still be associated with  $\Delta$ . Another goal was to study the hot carrier effect to control the effective activation energy ( $\Delta'$ ) of photodetectors and to analyze efficient energy transfer between hot carriers and cold carriers. Then iteratively improve the performance to obtain detector optimization.

The expected detector would have an advantage in terms of a lower dark current with a given photoresponse threshold wavelength. The operation of the photodetector involves three stages: 1) Injection of hot carriers through the barrier to the absorber. 2) Interaction of injected hot carriers with the cold carriers into the absorber, exchanging of energy and formation of a quasi-Fermi level at a hot hole temperature greater than the lattice temperature. 3) The excitation of the hot holes by absorption of longer wavelength photon from the quasi-Fermi distribution.

**Accomplishments:** We have designed several extended threshold detectors, where the design threshold wavelength is much shorter than the experimentally observed wavelength threshold. We have also shown that the extended threshold dark currents are governed by the designed (longer wavelength Threshold). Several Samples were grown (SP 1001, SP 1007, 15SP3, HE 0204, LH 1002, SP1, SP2).

- 1) Dark current of the extended threshold device was fitted to a modelled device showing that it matches with a device with the longer energy gap or shorter wavelength. A modelled device with the design threshold wavelength and also compared to the modelled device with a longer threshold wavelength to show that the extended threshold device has a lower dark current than the normal longer threshold detector. More details, (figures, device and performance parameters) are given in the report attached.
- 2) We also demonstrated that the device offset is essential to obtain the extended threshold wavelength.
- 3) we also demonstrated that the grade barrier will enhance the threshold wavelength extension.
- 4) A basic empirical model for the hot carrier effects in the extended threshold detector is also proposed.

## RPPR Final Report as of 05-Dec-2022

Could not test the ideas for the hot carrier effects based on the empirical model, due to the shut down of the labs not only at GSU but also world wide, affecting our collaboration with university of LEEDS where we receive the samples.

**Training Opportunities:** Four Ph.D. students completed their studies during this period. One MS student also completed his MS thesis. All of those trained are contributing towards improving the US technological advances. Graduate and postdoctoral trainees' present positions are listed and most of the undergraduates have joined either graduate programs or entered the commercial entities and some of them have enlisted in US government agencies such as Central Intelligence Agency (CIA).

- Dr. Jito Titus: Ph.D. completed December 2016, VP of Research and Development, RCE technologies, Carlsbad CA.
- Dr. Seyoum Wolde: Ph.D. completed Jan 2018, Lecturer at Georgia State University, Perimeter campus
- Dr. Dilip Chauhan: Ph.D. completed Dec 2018, Process Development Engineer, Intel Corporation, Albuquerque, New Mexico.
- Dr. Hemendra Ghimire: Ph.D. completed May 2021, Postdoctoral Associate, City of Hope National Medical Center, Duarte, CA.
- Mr. Dimuthu Bandara Obeysekara: MS Completed summer 2016. (Graduate Assistant: New Jersey Institute of Technology)

Several Postdoctoral Associates were also trained in the Optoelectronics laboratory:

- Dr. Yang Feng Lao: Director, Product & Engineering, Hisense Chip BU, South Plainfield, New Jersey.
- S. Kabi: Assistant Professor, University of Calcutta, India
- Dr. Divya Somvanshi: Assistant Professor, Department of Physics, HBTU, Kanpur, India
- Dr. Tae Young Park: back in Korea

Several undergraduates both from Georgia State and other surrounding Universities participated in research activities at the optoelectronics laboratory. Mentored Associate Professor Landewatte Ajith De Silva from the University of West Georgia during his leave of absence from UWG in the summer of 2018 and in the Fall of 2018. In addition, he also had several of his undergraduate students performing part of the research in the optoelectronics Laboratory. Dr. Mathes Dayananda, An Associate professor of Physics at Georgia State University, Dunwoody campus is also participating in our research work with several of his undergraduate students.

- Mentored an Assistant Professor Gouying Yan from Hebei University China through the GSU Faculty Mentoring Program (FMP) organized by the Office of International Initiatives. (Spring 2017)
- GSU undergraduates: Joshua Stanley, Samuel Orlando Core, Gay James, Saina Ahmadpour, Shad Huda, Nicolette Venant. Okiche Sharon, Louis Ramos
- GSU Dunwoody campus undergraduates: Nathan G Grodzinsky, Hikma Adams
- Mentored an undergraduate Hongmei Zhang from Hebei University China through the GSU Summer Institute. (Summer 2017)
- University of West Georgia (UWG) undergraduates: Ryan Landry, Nicole Morris, Sarah Nazaret, Victoria Martins, Susie Machado

## RPPR Final Report as of 05-Dec-2022

**Results Dissemination:** Special Issue “Semiconductor Infrared Devices and Applications” A special issue of Editor for the open access journal Micromachines (ISSN 2072-666X, ISBN 978-3-0365-3354-4 (PDF)), MDPI, Switzerland, 2020.

Conference presentations:

- "Infrared for healthy living" Georgia academy of science annual Conference, 2021 April 16-18,
- “Quantification of Infrared Spectral Markers for Ulcerative Colitis Using Sera”, SPIE BIOS, 3 February 2020, San Francisco, CA.
- “Threshold wavelength extension with dark current reduction in infrared detectors”, SPIE (2019 August 11-15) Infrared Remote Sensing and Instrumentation XXVII, San Diego. (INVITED)
- “Carbon based materials for hole- extraction in perovskite solar cells”, Poster Presentation, Materials Research Society, Fall Meeting 2021, A Hybrid Event, November 29 - December 08, 2021 presented by Ajith DeSilva .
- “Longitudinal analysis of molecular alteration in Serum samples of colitis mice by using Infrared Radiation for Healthy Living: Disease Diagnostics” A. G. U. Perera, Georgia Academy of Sciences, Annual Meeting, (Key Note Lecture) University of West Georgia, Carrollton, GA, April 13 2018.
- “Longitudinal analysis of molecular alteration in Serum samples of colitis mice by using Infrared Radiation for Healthy Living: Disease Diagnostics” Quantum Structure Infrared Photodetectors (QSIP 2018), Stockholm, Sweden, June 16-21, 2018.
- “Study of infrared photodetectors with wavelength extension Mechanism” Quantum Structure Infrared Photodetectors (QSIP 2018), Stockholm, Sweden, June 16-21, 2018. (INVITED)
- “STUDY OF EXTENDED WAVELENGTH INFRARED DETECTION ON PGAAS/ALGAAS HETEROSTRUCTURES”, Presented at the Georgia Academy of Sciences, April 14, 2018, University of West Georgia, Carrollton, GA. Presented by Dilip Chauhan.
- “Disease diagnostics with infrared spectroscopy of serum samples” Presented by Hemendra M Ghimire in the MBD meeting as a fellow on February 15, 2018.
- “Early Detection of Cell Activation by FTIR/ATR spectroscopy”, Presented at the Georgia Academy of Sciences, April 14, 2018, University of West Georgia, Carrollton, GA. Presented by Hemendra Mani Ghimire.
- “Anti-colitis drug signature monitoring via infrared spectroscopy” Presented by Hemendra M Ghimire in the MBD meeting as a fellow on October 27, 2018.
- “FIXING STOICHIOMETRY OF CUI FOR CONTROLLED MEASUREMENTS OF SEMICONDUCTING PROPERTIES” Presented at the Georgia Academy of Sciences, April 14, 2018, University of West Georgia, Carrollton, GA. Presented by Nicole Morris.
- “BRAGG MIRROR BASED ON ALQ3/TIO2 MULTILAYERS”, Presented at the Georgia Academy of Sciences, April 14, 2018, University of West Georgia, Carrollton, GA. Presented by Saran Nazaret.
- “Diagnostics Using Infrared Spectroscopy” International Conference on Sensing Technology (ICST 2017), Sydney, Australia, Dec 4-6, 2017. (INVITED)
- “Heterojunction detectors for multi-band detection with a wavelength threshold extension mechanism” International Conference and Exhibition on Lasers, Optics & Photonics, Las Vegas, USA, Nov15 -17, 2017. (INVITED)
- “Infrared spectroscopy as a screening technique for colitis”, Conference on “Bio-MEMS and Medical Microdevices III”, May 8-10 2017, Barcelona, Spain.
- "p-GaAs/AlGaAs heterostructures with a current blocking barrier for mid-infrared detection", AVS 63rd International Symposium & Exhibition, November 6-11, 2016, Music City Center, Nashville, Presented by Dilip Chauhan.
- “Mid-Infrared detection in p-GaAs/AlGaAs heterostructures with a current blocking barrier”, Fourth Conference on Sensors, MEMS and Electro-Optic Systems, 12-14 September, 2016, Skukuza, South Africa.
- "Extended threshold photo-detection in GaAs/AlGaAs split-off detectors at high temperatures" International Conference on Electronic Materials (IUMRS-ICEM 2016), July 4 - 8, 2016, Nanyang Technological University, Singapore. (INVITED)
- “Group III-nitride Heterojunction Based Multi-Band Detector on Si (111) Substrate Grown by Plasma Assisted Molecular Beam Epitaxy (PA-MBE)”, International Conference on Electronic Materials (IUMRS-ICEM 2016), July 4 - 8, 2016, Nanyang Technological University, Singapore., (INVITED)
- Materials (IUMRS-ICEM 2016), July 4 - 8, 2016, Nanyang Technological University, Singapore., (INVITED)
- “Infrared photodetectors with wavelength extension beyond the spectral limit” SPIE Defense and Security Symposium, April 17-21, 2016, Baltimore, Maryland, USA. (INVITED)
- Biological Screening Using Infrared Spectroscopy”, Presented at the Molecular Basis of Diseases Area of Focus (MBDAF), GSU, and Jan 21 2016. Presented by Jitto Titus.

## RPPR Final Report as of 05-Dec-2022

- “Infrared Spectroscopy: A Potential Screening Tool for Colitis” presented at the Digestive Disease Research Group (DDRG) at the Institute for Biomedical Sciences, GSU. Jan 2016. Presented by Jitto Tittus.
- “Hot Carrier Photodetectors”, International Conference on Microwave and Photonics (ICMAP - 2015), December 11- 13, 2015, Indian School of Mines, Dhanbad, India. Dec 11-13, 2015. (INVITED KEYNOTE SPEECH)
- “Temperature Dependent Internal Photoemission Spectroscopic (TDIPS) Probe for Band-offset studies”, II-VI Conference, October 7-10, 2015, Chicago, IL. (INVITED)
- “Tunable hot-carrier photodetectors”, AITA 2015 - Advanced Infrared Technology and Applications, Pisa, Italy, Sept 29 – Oct 02, 2015. (INVITED).
- “Hot Carrier Infrared Photodetectors”, IEEE Summer Topicals Meeting on Mid Infrared Photonics, July 13-15, 2015, Nassau, Bahamas. (INVITED)
- “Tunable hot-carrier photodetectors for terahertz frequency operation”, 26th International Symposium on Space Terahertz Technology, March 16-18, 2015, Harvard University, Cambridge, MA.
- “Hot-Carrier Photodetector beyond spectral limit”, 2014 Workshop on Innovative Nanoscale Devices and Systems (WINDS), November 30 – December 5, 2014, Kohala Coast, Hawaii, USA.
- “InAs/GaAs p-type quantum dot and dots-in-well infrared photodetectors”, OSA Topical Conference: AOM 2014 – The 4th Advances in Optoelectronics and Micro/nano-optics, September 18-20, 2014, Xian, China. (INVITED)
- “InAs/GaAs p-type quantum dot and dots-in-well infrared photodetectors” The 14th International Conference on Nanotechnology (IEEE NANO 2014), 33 Gerrard Street West Toronto, ON, Canada, August 18-21, 2014.

### Presentations at other Institutes/Universities

- Infrared detectors for Safe and Healthy Living”, Cleveland, Ohio, IEEE Chapter, September 23, 2021.
  - “Minimally invasive disease detection using ATR-FTIR Spectroscopy”, Mobile, Alabama IEEE Photonics Society, October 14 th 2021.
  - “Optoelectronics- History of Electronics leading to Infrared Detectors”, Department of Physics- University of South Alabama, October 14th 2021
  - “Minimally invasive disease detection using ATR-FTIR Spectroscopy”, presented to Boston Chapter of IEEE Photonics Society, April 8th 2021.
  - “Optoelectronics- History of Electronics leading to Infrared Detectors”, presented to Indian Institute of Technology - Varanasi, IEEE Photonics Society Student chapter March 18th 2021. (Virtual)
  - “Minimally invasive disease detection using ATR-FTIR Spectroscopy”, presented to University of Warsaw, Poland IEEE Photonics Society Student chapter ,March 10th 2021. (Virtual)
  - “Minimally invasive disease detection using ATR-FTIR Spectroscopy”, presented to University of Dayton, Ohio IEEE Photonics Society Student chapter, February 12th 2021. (Virtual)
- 43 refereed journal articles and three invited book chapters were also published enhancing the dissemination activities. [http://www.physics.gsu.edu/perera/papers/papers\\_outline.html](http://www.physics.gsu.edu/perera/papers/papers_outline.html)

**Honors and Awards:** “IEEE Photonics Society Distinguished Lecture Award – 2020-2021”: IEEE Photonics Society Distinguish Lecture Award 2020-2021. Re appointed for 2021-2022.

Fellow – Institute of Electrical and Electronics Engineers (IEEE) – 2012-present

Fellow - Photonics Society, IEEE 2016- present

Fellow – Society of Photo Instrumentation Engineers (SPIE) – 2009 -Present

Fellow – American Physical Society – 2006 - Present

Member of the Editorial Board - IEEE journal of Electron Device Society - 2016- 2022

Our Student(s) : Hemendra Mani Ghimire won the GSU Dissertation Award 2020-2021

Selected as the Most Outstanding Physics graduate of the Year - 2020

Selected as the best Molecular Basis of Disease (MBD) Fellow 2019-2020,  
2020-2021

JittoTittus selected as the Best presenter at the MBD Fellows Seminar three years in a row ,  
2015-16, -2016-17 and 2017- 8

**Protocol Activity Status:**

## RPPR Final Report as of 05-Dec-2022

**Technology Transfer:** Detection of Melanoma and Lymphoma by ATR-FTIR spectroscopy", (A. G. U. Perera, H. Ghimire), US Patent No.: US 2020/0056991 A1, application published on Feb. 20,2020.

Tunable Hot Carrier Photodetector" (A. G. U. Perera and Y. F. Lao), U.S. Patent No.: US 10,347,783 B2, issued on Jul. 9, 2019.

"Tunable Hot Carrier Photodetector" (A. G. U. Perera and Y. F. Lao), AU. Patent No.: AU 2014347256 B2, issued on Nov. 22, 2018.

Early Detection Of Cell Activation By ATR-FTIR Spectroscopy", (J. Titus, C. Filfli, A. G. U. Perera, J. K. Hilliard)U. S. Patent No. 99823129 B2, issued on May 29, 2018.

ATR-FTIR for Non-Invasive Detections of Colitis (A. G. U. Perera, J. Titus, D. Merlin, and E. Viennois), U.S. Patent No. 10527544 B2, issued on Jan 7, 2020

High Operation Temperature Split-Off Band Infrared Detectors", (A. G. U. Perera, S. G. Matsik, H. C. Liu) Canada Patent # CA 2662526 A1, issued on 12/22/2015.

### PARTICIPANTS:

**Participant Type:** PD/PI

**Participant:** Unil A. G. Perera

**Person Months Worked:** 1.00

Project Contribution:

National Academy Member: N

**Funding Support:**

**Participant Type:** Postdoctoral (scholar, fellow or other postdoctoral position)

**Participant:** Lao Feng Yan

**Person Months Worked:** 12.00

Project Contribution:

National Academy Member: N

**Funding Support:**

**Participant Type:** Postdoctoral (scholar, fellow or other postdoctoral position)

**Participant:** Sanjib Kabi

**Person Months Worked:** 12.00

Project Contribution:

National Academy Member: N

**Funding Support:**

**Participant Type:** Postdoctoral (scholar, fellow or other postdoctoral position)

**Participant:** Diviya Somvanshi

**Person Months Worked:** 11.00

Project Contribution:

National Academy Member: N

**Funding Support:**

**Participant Type:** Postdoctoral (scholar, fellow or other postdoctoral position)

**Participant:** Tae Young Park

**Person Months Worked:** 3.00

Project Contribution:

National Academy Member: N

**Funding Support:**

**RPPR Final Report**  
as of 05-Dec-2022

**Participant Type:** Graduate Student (research assistant)  
**Participant:** Jitto Titus  
**Person Months Worked:** 6.00 **Funding Support:**  
Project Contribution:  
National Academy Member: N

**Participant Type:** Graduate Student (research assistant)  
**Participant:** Dilip Chahuan  
**Person Months Worked:** 4.00 **Funding Support:**  
Project Contribution:  
National Academy Member: N

**Participant Type:** Graduate Student (research assistant)  
**Participant:** Seyoum Wolde  
**Person Months Worked:** 6.00 **Funding Support:**  
Project Contribution:  
National Academy Member: N

**Participant Type:** Graduate Student (research assistant)  
**Participant:** Dimuthu Obeysekara  
**Person Months Worked:** 6.00 **Funding Support:**  
Project Contribution:  
National Academy Member: N

**Participant Type:** Undergraduate Student  
**Participant:** Sarahn Nazaret  
**Person Months Worked:** 3.00 **Funding Support:**  
Project Contribution:  
National Academy Member: N

**Participant Type:** Undergraduate Student  
**Participant:** Nicole Morris  
**Person Months Worked:** 3.00 **Funding Support:**  
Project Contribution:  
National Academy Member: N

**Participant Type:** Graduate Student (research assistant)  
**Participant:** Bryan Lovaeil  
**Person Months Worked:** 3.00 **Funding Support:**  
Project Contribution:  
National Academy Member: N

**RPPR Final Report**  
as of 05-Dec-2022

**Participant Type:** Graduate Student (research assistant)

**Participant:** Seyoum Wolde

**Person Months Worked:** 9.00

**Funding Support:**

Project Contribution:

National Academy Member: N

**International Collaboration:**

GBR  
GBR  
LKA  
CHN

LKA

**ARTICLES:**

**Publication Type:** Journal Article      Peer Reviewed: Y      **Publication Status:** 1-Published

**Journal:** Progress in Quantum Electronics

Publication Identifier Type: DOI

Publication Identifier: 10.1016/j.pquantelec.2016.05.001

Volume: 48

Issue: 0

First Page #: 1

Date Submitted: 8/8/18 12:00AM

Date Published: 3/13/16 9:00AM

Publication Location: NY, NY

**Article Title:** Heterojunction and Superlattice detectors for Infrared to Ultraviolet”

**Authors:** A. G. U. Perera

**Keywords:** Type II Superlattice Detectors, Heterojunction

**Abstract:** The interest in Infrared and Ultraviolet detectors has increased immensely due to the emergence of important applications over a wide range of activities. Detectors based on free carrier absorption known as Hetero-junction Interfacial Workfunction Internal Photoemission (HEIWIP) detectors and variations of these heterojunction structures to be used as intervalence band detectors for a wide wavelength region are presented. Although this internal photoemission concept is valid for all semiconductor materials systems, using a well studied III-V system of GaAs/Al<sub>x</sub>Ga<sub>1-x</sub>As to cover a wide wavelength range from UV to far-infrared (THz) is an important development in detector technology. Using the intervalence band (heavy hole, light hole and split off) transitions for high operating temperature detection of mid Infrared radiation is also discussed. A promising new way to extend the detection wavelength threshold beyond the standard threshold connected with the energy gap in a GaAs/Al<sub>x</sub>Ga<sub>1-x</sub>As

**Distribution Statement:** 3-Distribution authorized to U.S. Government Agencies and their contractors

Acknowledged Federal Support: Y

## RPPR Final Report as of 05-Dec-2022

**Publication Type:** Journal Article Peer Reviewed: Y **Publication Status:** 1-Published

**Journal:** Optics Letters

Publication Identifier Type: DOI

Publication Identifier: 10.1364/OL.41.000285

Volume: 41

Issue: 2

First Page #: 285

Date Submitted: 8/8/18 12:00AM

Date Published: 1/15/16 10:00AM

Publication Location: NY, NY

**Article Title:** Mid-infrared photodetectors with extended wavelength operation at high temperatures

**Authors:** Y.F. Lao, A. G. Unil Perera, L.H. Li, S.P. Khanna, E. H. Linfield, Y. H. Zhang, T. M. Wang

**Keywords:** Extended Wavelength, high operating temperature

**Abstract:** We report a threshold extension, from the designed value of 3.1  $\mu\text{m}$  to 8.9  $\mu\text{m}$  in a p-type heterostructure photodetector. This is associated with the use of a graded barrier and barrier offset, which leads to hot carrier interactions. Experiments show that use of long-pass filters tunes the energies of incident photons, giving rise to the change in response threshold. This study demonstrates an alternative approach to achieve tuning photodetector response without the need to adjust the photodetector's characteristic energy which is determined by the band structure.

**Distribution Statement:** 3-Distribution authorized to U.S. Government Agencies and their contractors

Acknowledged Federal Support: Y

**Publication Type:** Journal Article Peer Reviewed: Y **Publication Status:** 1-Published

**Journal:** Advances in Optoelectronics

Publication Identifier Type: DOI

Publication Identifier: 10.1155/2016/1832097

Volume: 2016

Issue: 0

First Page #: 0

Date Submitted: 8/8/18 12:00AM

Date Published: 2/1/16 3:00PM

Publication Location: NY, NY

**Article Title:** Physics of Internal Photoemission and Its Infrared Applications in the Low-Energy Limit

**Authors:** Y. F. Lao, A. G. U. Perera

**Keywords:** TDIPS, Band OFFsets, II-V, II-VI

**Abstract:** Internal photoemission (IP) correlates with processes in which carriers are photoexcited and transferred from one material to another. This characteristic allows characterizing the properties of the heterostructure, for example, the band parameters of a material and the interface between two materials. IP also involves the generation and collection of photocarriers, which leads to applications in the photodetectors. This review discusses the generic IP processes based on heterojunction structures, characterizing  $n$ -type band structure and the band offset at the heterointerface, and infrared photodetection including a novel concept of photoresponse extension based on an energy transfer mechanism between hot and cold carriers.

**Distribution Statement:** 3-Distribution authorized to U.S. Government Agencies and their contractors

Acknowledged Federal Support: Y

**Publication Type:** Journal Article Peer Reviewed: Y **Publication Status:** 1-Published

**Journal:** Applied Physics Letters

Publication Identifier Type: DOI

Publication Identifier: 10.1063/1.4952431

Volume: 108

Issue: 20

First Page #: 201105

Date Submitted: 8/8/18 12:00AM

Date Published: 5/19/16 8:00AM

Publication Location: NY, NY

**Article Title:** Effect of a current blocking barrier on a 2–6  $\mu\text{m}$  p-GaAs/AlGaAs heterojunction infrared detector

**Authors:** D. Chauhan, A. G. U. Perera, L.H. Li, L. Chen, E. H. Linfield

**Keywords:** Current blocking, graded barrier, multiperiod, uncooled, heterostructure IR detectors

**Abstract:** We report the performance of a 30 period p-GaAs/Al<sub>x</sub>Ga<sub>1-x</sub>As heterojunction photovoltaic infrared detector, with graded barriers, operating in the 2–6  $\mu\text{m}$  wavelength range. Implementation of a current blocking barrier increases the specific detectivity ( $D^*$ ) under dark conditions by two orders of magnitude to  $1.9 \times 10^{11}$  Jones at 2.7  $\mu\text{m}$ , at 77K. Furthermore, at zero bias, the resistance-area product (ROA) attains a value of  $17.2 \times 10^8 \Omega \text{cm}^2$ , a five orders enhancement due to the current blocking barrier, with the responsivity reduced by only a factor of 1.5.

**Distribution Statement:** 3-Distribution authorized to U.S. Government Agencies and their contractors

Acknowledged Federal Support: Y

## RPPR Final Report as of 05-Dec-2022

**Publication Type:** Journal Article Peer Reviewed: Y **Publication Status:** 1-Published

**Journal:** Journal of Biophotonics

Publication Identifier Type: DOI

Publication Identifier: 10.1002/jbio.201600041

Volume: 10

Issue: 0

First Page #: 465

Date Submitted: 8/8/18 12:00AM

Date Published: 4/21/16 12:00PM

Publication Location: Weinheim, Germany

**Article Title:** Minimally invasive screening for colitis using attenuated total internal reflectance fourier transform infrared spectroscopy

**Authors:** J. Titus, E. Viennois, D. merlin, A. G., U. Perera

**Keywords:** colitis, ATR-FTIR, sera, screening, minimally invasive

**Abstract:** This article describes a rapid, simple and cost-effective technique that could lead to a method for detecting colitis without the need for biopsies or in vivo measurements. The detection technique includes the testing of blood serum using Attenuated Total Reflectance Fourier Transform Infrared (ATR-FTIR) spectroscopy for the colitis-induced increased presence of mannose. The reference or the baseline spectrum can be the pooled and averaged spectra of non-colitic samples or the subject's previous sample spectrum allowing for personalized diagnosis and drug management.

**Distribution Statement:** 3-Distribution authorized to U.S. Government Agencies and their contractors

Acknowledged Federal Support: Y

**Publication Type:** Journal Article Peer Reviewed: Y **Publication Status:** 1-Published

**Journal:** Journal of Applied Physics

Publication Identifier Type: DOI

Publication Identifier: 10.1063/1.4943591

Volume: 119

Issue:

First Page #: 105304

Date Submitted: 7/22/16 12:00AM

Date Published: 7/22/16 2:10PM

Publication Location: Ny, NY

**Article Title:** Optical characteristics of p-type GaAs-based semiconductors towards applications in photoemission infrared detectors

**Authors:** Y. F. Lao, A. G. U. Perera, H. L. Wang, J. H. Zhao, Y. J. Jin, D. H. Zhang

**Keywords:** Optocal Characteristics, Photoemiision, Infrared Detectors, II- V materials

**Abstract:** Free-carrier effects in a p-type semiconductor including the intra-valence-band and inter-valence-band optical transitions are primarily responsible for its optical characteristics in infrared. Attention has been paid to the inter-valence-band transitions for the development of internal photoemission (IPE) mid-wave infrared (MWIR) photodetectors. The hole transition from the heavy-hole (HH) band to the spin-orbit split-off (SO) band has demonstrated potential applications for 3–5  $\mu\text{m}$  detection without the need of cooling. However, the forbidden SO-HH transition at the C point (corresponding to a transition energy  $D_0$ , which is the split-off gap between the HH and SO bands) creates a sharp drop around 3.6  $\mu\text{m}$  in the spectral response of p-type GaAs/AlGaAs detectors. Here, we report a study on the optical characteristics of p-type GaAs-based semiconductors, including compressively strained InGaAs and GaAsSb, and a dilute magnetic semiconductor, GaMnAs. A model-independent fitting

**Distribution Statement:** 3-Distribution authorized to U.S. Government Agencies and their contractors

Acknowledged Federal Support: Y

## RPPR Final Report as of 05-Dec-2022

**Publication Type:** Journal Article Peer Reviewed: Y **Publication Status:** 1-Published

**Journal:** Optical Engineering

Publication Identifier Type: DOI

Publication Identifier: 10.1117/1.OE.56.9.091605

Volume: 56

Issue: 9

First Page #: 091605

Date Submitted: 6/16/17 12:00AM

Date Published: 2/7/17 3:00PM

Publication Location: Bellingham, Washington

**Article Title:** Extended wavelength infrared photodetectors",

**Authors:** D. Chauhan, A. G. U. Perera, L. H. Li, L. Chen, S. P. Khanna, and E. H. Linfield,

**Keywords:** Extended threshold, Infrared Detectors, Offset

**Abstract:** Extension of the wavelength threshold of an infrared detector beyond  $\frac{1}{2} hc$  is demonstrated, without reducing the minimum energy gap ( $E_g$ ) of the material. Specifically, a photodetector designed with  $E_g = 0.40$  eV, and a corresponding  $\lambda_c = 3.1 \mu\text{m}$ , was shown to have an extended threshold of  $\lambda_c = 4.5 \mu\text{m}$  at 5.3 K, at zero bias. Under negative and positive applied bias, this range was further extended to  $\lambda_c = 6.0$  and  $\lambda_c = 6.8 \mu\text{m}$ , respectively, with the photoresponse becoming stronger at increased biases, but the spectral threshold remained relatively constant. The observed wavelength extension arises from an offset between the two potential barriers in the device. Without the offset, another detector with  $E_g = 0.30$  eV showed a photoresponse with the expected wavelength threshold of  $\lambda_c = 4 \mu\text{m}$ .

**Distribution Statement:** 3-Distribution authorized to U.S. Government Agencies and their contractors

Acknowledged Federal Support: Y

**Publication Type:** Journal Article Peer Reviewed: Y **Publication Status:** 1-Published

**Journal:** Journal of Applied Physics

Publication Identifier Type: DOI

Publication Identifier: 10.1063/1.4989834]

Volume: 121

Issue:

First Page #: 244501

Date Submitted: 8/6/18 12:00AM

Date Published: 8/15/17 8:00AM

Publication Location: New Yourk, NY

**Article Title:** Noise, Gain, and Capture probability of p-type InAs-GaAs Quantum-Dot and Quantum Dot-in-well Infrared Photodetectors

**Authors:** Seyoum Wolde<sup>1</sup>, Yan-Feng Lao<sup>1,b</sup>, A. G. Unil Perera<sup>1,a</sup>, Y. H. Zhang<sup>2</sup>, T. M. Wang<sup>2</sup>, J. O. Kim<sup>3</sup>, Ted S

**Keywords:** Quantum dot, Noise, Gain, Capture probability.

**Abstract:** We report experimental results showing how the noise in a Quantum-Dot Infrared photodetector (QDIP) and Quantum Dot-in-a-well (DWELL) vary with the electric field and temperature. At lower temperatures (below  $\sim 100$  K), the noise current of both types of detectors are dominated by generation-recombination (G-R) noise which is consistent with a mechanism of fluctuations driven by the electric field and by thermal noise. The noise gain, capture probability and carrier life time for bound-to-continuum or quasi-bound transitions in DWELL and QDIP structures are discussed. The capture probability of DWELL is found to be more than two times higher than the corresponding QDIP. Based on the analysis, structural parameters such as the numbers of active layers, the surface density of QDs, and the carrier capture or relaxation rate, type of material and electric field are some of the optimization parameters identified to improve the gain of devices.

**Distribution Statement:** 3-Distribution authorized to U.S. Government Agencies and their contractors

Acknowledged Federal Support: Y

## RPPR Final Report as of 05-Dec-2022

**Publication Type:** Journal Article      Peer Reviewed: Y      **Publication Status:** 1-Published  
**Journal:** Journal of Applied Physics  
**Publication Identifier Type:** DOI      **Publication Identifier:** 10.1364/OL.41.000285  
**Volume:** 41      **Issue:** 2      **First Page #:** 285  
**Date Submitted:** 8/6/18 12:00AM      **Date Published:**  
**Publication Location:**

**Article Title:** Dark current and photoresponse characteristics of extended wavelength infrared photodetectors

**Authors:** D. Chauhan,<sup>1</sup> A. G. U. Perera,<sup>1, a)</sup> L. H. Li,<sup>2</sup> L. Chen,<sup>2</sup> and E. H. Linfield<sup>2</sup>

**Keywords:** Infrared detectors, hot carriers, extended wavelength, GaAs/AlGaAs

**Abstract:** The dark current and spectral photoresponse threshold of a semiconductor photodetector are normally determined by the minimum energy gap (?) of the material, or the interfacial energy gap of the heterostructure. In this manuscript, we discuss the performance of an asymmetric p-GaAs/Al<sub>x</sub>Ga<sub>1-x</sub>As heterostructure-based infrared photodetector, which shows an extended wavelength threshold beyond the limit set by ?. The measured dark current was found to agree well with fits obtained from a 3D carrier drift model using the designed value of ? ~0.40 eV (~3.1 μm). In contrast, the spectral photoresponse showed extended wavelength thresholds of ~68 μm, ~45 μm, and ~60 μm at positive, zero, and negative biases, respectively, at 5.3K. For a reference (symmetric) photodetector, the dark current was fitted with the designed value of ? ~0.30 eV, and excellent agreement was obtained for both the measured dark current and spectral response. This underlies the advantage of using asymmetric infrared phot

**Distribution Statement:** 3-Distribution authorized to U.S. Government Agencies and their contractors  
**Acknowledged Federal Support:** Y

**Publication Type:** Journal Article      Peer Reviewed: Y      **Publication Status:** 1-Published  
**Journal:** IEEE J selected topics of Quantum Electronics  
**Publication Identifier Type:** DOI      **Publication Identifier:** 10.1109/JSTQE.2017.2773622,  
**Volume:**      **Issue:**      **First Page #:**  
**Date Submitted:** 8/6/18 12:00AM      **Date Published:**  
**Publication Location:**

**Article Title:** Analysis of Extended Threshold Wavelength Photoresponse in Non-symmetrical p-GaAs/AlGaAs Heterostructure Photodetectors

**Authors:** D. Somvanshi, D. Chauhan, Y.-F. Lao, A. G. Unil Perera, Fellow, IEEE, L. H. Li, S. P. Khanna and E. H.

**Keywords:** quasi-Fermi distribution, threshold photoresponse, non-symmetrical, temperatre.

**Abstract:** We analyze the extended wavelength photoresponse beyond the standard threshold limit ( , where is the activation energy) in non-symmetrical p-GaAs/AlGaAs heterostructure photodetectors with a barrier energy offset. We propose that hot-cold hole carrier interactions in the p-GaAs absorber are responsible for the threshold wavelength extension. Experimental results are analyzed by considering a quasi-Fermi distribution of hot holes at a hot hole temperature , which is much higher than the lattice temperature . The experimental photoresponse is fitted using an escape cone model, modified with a quasi-Fermi level (EquasiF). The simulated results are found to be in good agreement with experimental data, justifying the model used.

**Distribution Statement:** 3-Distribution authorized to U.S. Government Agencies and their contractors  
**Acknowledged Federal Support:** Y

## RPPR Final Report as of 05-Dec-2022

**Publication Type:** Journal Article Peer Reviewed: Y **Publication Status:** 1-Published

**Journal:** J Biophotonics

Publication Identifier Type: DOI

Publication Identifier: 10.1002/jbio.201700057

Volume: Issue:

First Page #:

Date Submitted: 8/8/18 12:00AM

Date Published: 12/4/17 5:00AM

Publication Location:

**Article Title:** Protein secondary structure analysis of dried blood serum using infrared spectroscopy to identify markers for colitis screening

**Authors:** Jitto Titus<sup>1</sup>, Hemendra Ghimire<sup>1</sup>, Emilie Viennois<sup>2,3</sup>, Didier Merlin<sup>2,3,4</sup> and A. G. Unil Perera<sup>1</sup>,

**Keywords:** ATR-FTIR, Sera, anti-TNF-alpha, Secondary structure

**Abstract:** There remains a great need for diagnosis of inflammatory bowel disease (IBD), for which the current technique, colonoscopy, is costly and also has risks for complications. Attenuated Total Reflectance Fourier Transform Infrared (ATR-FTIR) spectroscopy is a new screening technique to evaluate colitis. Using second derivative spectral deconvolution of the absorbance spectra, a full set of spectral markers were identified based on statistical analysis. Using this method, Amide I group frequencies, (specifically, alpha helix to beta sheet ratio of the protein secondary structure) were identified in addition to the previously reported glucose and mannose signatures in sera of chronic and acute mice models of colitis. We also used the same technique to demonstrate that these spectral markers (alpha helix/beta sheet ratio, glucose and mannose) are recovering to basal levels upon Anti-TNF $\alpha$  therapy. Hence, this technique will be able to identify changes in the sera due to diseases.

**Distribution Statement:** 3-Distribution authorized to U.S. Government Agencies and their contractors  
Acknowledged Federal Support: Y

**Publication Type:** Journal Article Peer Reviewed: Y **Publication Status:** 1-Published

**Journal:** SPIE Proceedings

Publication Identifier Type:

Publication Identifier:

Volume: Issue:

First Page #:

Date Submitted: 6/16/17 12:00AM

Date Published:

Publication Location:

**Article Title:** Mid-Infrared detection in p-GaAs/AlGaAs heterostructures with a current blocking barrier

**Authors:** Dilip Chauhan<sup>1</sup>, A. G. Unil Perera<sup>1,\*</sup>, Lianhe Li<sup>2</sup>, Li Chen<sup>2</sup>, Edmund H. Linfield<sup>2</sup>

**Keywords:** Mid-infrared, current blocking barrier, GaAs/AlGaAs heterostructures.

**Abstract:** For the infrared detection in the 3-5  $\mu$ m range, p-GaAs/Al<sub>x</sub>Ga<sub>1-x</sub>As heterojunction is an attractive material system due to light hole/heavy hole and spin-orbit split-off intra-valance band transitions in this wavelength range. Varying the Al mole fraction (x) provides the tuning for the wavelength threshold, while graded Al<sub>x</sub>Ga<sub>1-x</sub>As potential barriers create an asymmetry to allow a photovoltaic operation. The photovoltaic mode of operation offers the advantage of thermal noise limited performance. In our preliminary work, a 2 – 6  $\mu$ m photovoltaic detector was studied. Implementation of an additional current blocking barrier improved the specific detectivity ( $D^*$ ) by two orders of magnitude, to  $1.9 \times 10^{11}$  Jones at 2.7  $\mu$ m, at 77K. At zero bias, the resistance-area product (ROA) had a value of  $\sim 7.2 \times 10^8 \Omega \text{ cm}^2$ , which is five orders higher in magnitude (with a corresponding reduction of the responsivity by only a factor of  $\sim 1.5$ ), compared to the ROA value without the blocking barrier. A photoresp

**Distribution Statement:** 3-Distribution authorized to U.S. Government Agencies and their contractors  
Acknowledged Federal Support: Y



## RPPR Final Report as of 05-Dec-2022

**Publication Type:** Journal Article      Peer Reviewed: Y      **Publication Status:** 1-Published

**Journal:** Scientific Reports

Publication Identifier Type: DOI

Publication Identifier: 10.1038/s41598-017-17027-4

Volume: 7

Issue: 1

First Page #:

Date Submitted: 8/8/18 12:00AM

Date Published: 12/1/17 5:00AM

Publication Location:

**Article Title:** ATR-FTIR spectral discrimination between normal and tumorous mouse models of lymphoma and melanoma from serum samples

**Authors:** Hemendra Ghimire, Mahathi Venkataramani, Zhen Bian, Yuan Liu, A. G. Unil Perera

**Keywords:** Spectral bio markers, ATR-FTIR Spectrsal discrimination, Lymphoma and Melanoma

**Abstract:** This study presents, attenuated total reflection Fourier transforms infrared spectroscopy of dried serum samples in an effort to assess biochemical changes induced by non-Hodgkin's lymphoma and subcutaneous melanoma. An EL4 mouse model of non-Hodgkin lymphoma and a B16 mouse model of subcutaneous melanoma are used to extract a snapshot of tumor-associated alteration in the serum. The study of both cancer-bearing mouse models in wild types and their corresponding control types, emphasizes the diagnostic potential of this approach as a screening technique for non-Hodgkin lymphoma and melanoma skin cancer. Infrared absorbance values of the different spectral bands, hierarchical clustering and integral values of the component bands by curve fitting, show statistically significant differences (student's t-test, two-tailed unequal variance p-value<0.05) between spectra representing healthy and tumorous mouse. This technique may thus be useful for having individualized route maps for rapid evaluation

**Distribution Statement:** 3-Distribution authorized to U.S. Government Agencies and their contractors

Acknowledged Federal Support: Y

**Publication Type:** Journal Article      Peer Reviewed: Y      **Publication Status:** 1-Published

**Journal:** Infrared Physics & TEchnology

Publication Identifier Type: DOI

Publication Identifier: <https://doi.org/10.1016/j.infrared.2018.10.007>

Volume: 95

Issue:

First Page #: 148

Date Submitted: 8/20/19 12:00AM

Date Published:

Publication Location: United States

**Article Title:** Study of infrared photodetectors with wavelength extension mechanism

**Authors:** D. Chauhan, A. G. U. Perera, L. H. Li, L. Chen, and E. H. Linfield

**Keywords:** Infrared photodetector, extended wavelength photoresponse, GaAs/AlGaAs heterostructure

**Abstract:** The III-V semiconductor heterostructure-based photodetectors have been studied extensively for infrared detection, from near-infrared (NIR) to far-infrared (FIR) region. Due to the mature material system, GaAs/Al<sub>x</sub>Ga<sub>1-x</sub>As heterostructures are attractive options for development of infrared detectors. The conventional rule of photodetection, determines the wavelength threshold (  $\lambda_c$  ) of spectral photoresponse, where  $\lambda_c$  is the minimum energy gap of the material, or the interfacial energy gap of the heterostructure. In recent studies on the p-GaAs/Al<sub>x</sub>Ga<sub>1-x</sub>As heterostructure-based infrared photodetectors, spectral threshold limit due to  $\lambda_c$  has been overcome owing to a detection mechanism arising from the hot-carrier effect driven extended wavelength photoresponse mechanism. It has been experimentally observed that a detector with a conventional spectral threshold of  $\sim 3.1 \mu\text{m}$  shows an extended wavelength threshold of up to  $\sim 68 \mu\text{m}$ . An important advantage of the wavelength extension mechanism.

**Distribution Statement:** 3-Distribution authorized to U.S. Government Agencies and their contractors

Acknowledged Federal Support: Y

## RPPR Final Report as of 05-Dec-2022

**Publication Type:** Journal Article Peer Reviewed: Y **Publication Status:** 1-Published

**Journal:** Infrared Physics and Technology

Publication Identifier Type: DOI

Publication Identifier: doi.org/10.1016/j.infrared.2018.11.034

Volume: 97

Issue:

First Page #: 33

Date Submitted: 7/15/20 12:00AM

Date Published: 3/29/20 12:00PM

Publication Location: Switzerland

**Article Title:** Longitudinal analysis of molecular alteration in serum samples of colitis mice by using infrared spectroscopy

**Authors:** Hemendra Ghimire, P. V. V Jayaweera, and A. G. Unil Perera

**Keywords:** Colitis, Infrared ATR spectroscopy, Longitudinal analysis, Mouse models, Serum

**Abstract:** The activation energy obtained from the temperature-dependent internal photoemission spectroscopy (TDIPS) and thermionic dark currents using GaAs/AlGaAs photodetectors is compared. P-type GaAs/AlGaAs heterostructures with different barrier heights are studied. The temperature-dependent spectral response shows the red-shifting of the detector threshold wavelength for increasing temperature due to the decreasing band-offset. The activation energy extracted from the Arrhenius plot of the dark current-voltage-temperature (I-V-T) and measured spectral response shows the carrier activation energy increases with increasing Al mole fraction and decreases with increasing doping density. For Infrared detectors with  $6.5\ \mu\text{m}$ , the Arrhenius analysis yields the values of activation energy with less than 5% deviation from the actual or TDIPS fitting values.

**Distribution Statement:** 2-Distribution Limited to U.S. Government agencies only; report contains proprietary info  
Acknowledged Federal Support: Y

**Publication Type:** Journal Article Peer Reviewed: Y **Publication Status:** 1-Published

**Journal:** Sensors Letters

Publication Identifier Type: DOI

Publication Identifier: 10.1109/LENS.2019.2915016

Volume: 3

Issue: 5

First Page #:

Date Submitted: 8/20/19 12:00AM

Date Published: 5/6/19 4:00AM

Publication Location: United States

**Article Title:** Reduced Dark Current With a Specific Detectivity Advantage in Extended Threshold Wavelength Infrared Detector

**Authors:** Divya Somvanshi, Dilip Chauhan, A. G. Unil Perera, Lianhe Li, Li Chen, and Edmund H. Linfield

**Keywords:** Electromagnetic wave sensors, dark current, detectivity, GaAs/AlGaAs heterostructures, infrared (IR) photodetectors, optoelectronic sensors.

**Abstract:** —Reduced dark current leading to a specific detectivity ( $D^*$ ) advantage over conventional detectors for extended threshold wavelength (ET) detectors are reported in this article. For an infrared (IR) detector with a graded injector barrier and barrier energy offset, the measured dark current was found to agree well with theoretical fits obtained from a 3-D carrier drift model using the designed value of  $\phi_b = 0.40\ \text{eV}$  ( $\lambda_t = 3.1\ \mu\text{m}$ ) (where  $\phi_b = 1.24/\lambda_t$ ,  $\phi_b$  is the internal work function and  $\lambda_t$  is the corresponding threshold wavelength), whereas the effective photoresponse threshold wavelength determined from the spectral response measurements corresponds to  $13.7\ \mu\text{m}$  at 50 K. However, for the conventional detectors, both the dark current and photoresponse threshold agree very well with the designed value of  $\phi_b$ . Comparing threshold wavelengths of an ET detector and a conventional detector, an advantage in  $D^*$  is observed for ET detectors due to the strong reduction in dark current.

**Distribution Statement:** 3-Distribution authorized to U.S. Government Agencies and their contractors  
Acknowledged Federal Support: Y

## RPPR Final Report as of 05-Dec-2022

**Publication Type:** Journal Article      Peer Reviewed: Y      **Publication Status:** 1-Published

**Journal:** Sensors Letters

Publication Identifier Type: DOI

Publication Identifier: 10.1109/LSENS.2018.2881047

Volume: 2

Issue: 4

First Page #:

Date Submitted: 8/20/19 12:00AM

Date Published: 11/28/18 10:00AM

Publication Location: United States

**Article Title:** Effects of Barrier Energy Offset and Gradient in Extended Wavelength Infrared Detectors

**Authors:** Dilip Chauhan, A. G. Unil Perera<sup>1</sup>, Lianhe Li, Li Chen, and Edmund H. Linfield

**Keywords:** Electromagnetic wave sensors, extended wavelength infrared (IR) photodetectors, GaAs/AlGaAs heterostructures, III-V semiconductors.

**Abstract:** The extended wavelength infrared (IR) photodetectors are the new class of III-V semiconductor heterojunctionbased photodetectors that can detect incoming radiation with energy significantly smaller than the minimum energy gap ( $E_g$ ) at the heterojunction interface. The architecture of these photodetectors includes a barrier-emitter-barrier epilayers sandwiched between highly doped ohmic top and bottom contact layers. An energy offset ( $\Delta E$ ) between the barriers is necessary for the extended wavelength photodetection. In this article, we study the performance of extended wavelength IR photodetectors with varying  $\Delta E$  and gradient of the potential barrier. Results indicate that the extended wavelength threshold varied slightly with varying both the gradient and offset. Spectral responsivity, however, increased with the increasing offset and decreased with increasing gradient.

**Distribution Statement:** 3-Distribution authorized to U.S. Government Agencies and their contractors

Acknowledged Federal Support: Y

**Publication Type:** Journal Article      Peer Reviewed: Y      **Publication Status:** 1-Published

**Journal:** Infrared Physics and Technology

Publication Identifier Type: DOI

Publication Identifier: 10.1016/j.infrared.2019.103026

Volume: 102

Issue:

First Page #: 103026

Date Submitted: 7/15/20 12:00AM

Date Published: 11/1/19 4:00PM

Publication Location: Netherlands

**Article Title:** Accuracy of activation energy from Arrhenius plots and temperature-dependent internal photoemission spectroscopy

**Authors:** Seyoum Wolde, Dilip Chauhan, Divya Somvanshi, A.G. Unil Perera, L.H. Li, Li Chen, S.P. Khanna, E.H.

**Keywords:** Activation Energy, Arrhenius Plot, Dark Current, Internal Photoemission, Temperature dependant internal Photoemission

**Abstract:** The activation energy obtained from the temperature-dependent internal photoemission spectroscopy (TDIPS) and thermionic dark currents using GaAs/AlGaAs photodetectors is compared. Different barrier heights within the p-type GaAs/AlGaAs heterostructures are studied. The temperature-dependent spectral response shows the red-shifting of the detector threshold wavelength for increasing temperature due to the decreasing band-offset. The activation energy extracted from the Arrhenius plot of the dark current-voltage-temperature (I-V-T) and measured spectral response shows the carrier activation energy increases with increasing Al mole fraction and decreases with increasing doping density. For Infrared detectors with  $\lambda_{th} \approx 6.5 \mu\text{m}$ , the Arrhenius analysis yields the values of activation energy with less than 5% deviation from the actual or TDIPS fitting values. However, for detectors with longer threshold wavelengths ( $\lambda_{th} \approx 9.3 \mu\text{m}$ ),

**Distribution Statement:** 2-Distribution Limited to U.S. Government agencies only; report contains proprietary info

Acknowledged Federal Support: Y



**RPPR Final Report**  
as of 05-Dec-2022

**Publication Type:** Conference Paper or Presentation **Publication Status:** 1-Published  
**Conference Name:** SPIE Defense + Commercial Sensing 2016  
Date Received: 16-Jun-2017 Conference Date: 17-Apr-2016 Date Published: 17-Apr-2016  
Conference Location: Baltimore, Maryland  
**Paper Title:** Infrared Photodetector with wavelength extension beyond the spectral limit  
**Authors:** A. G. U. Perera, D. Chauhan, Y. F. Lao, L.H. Li, S. P. Khanna, E. H. Linfield  
Acknowledged Federal Support: **Y**

**Publication Type:** Conference Paper or Presentation **Publication Status:** 1-Published  
**Conference Name:** SMEOS 2016  
Date Received: 16-Jun-2017 Conference Date: 12-Sep-2016 Date Published: 12-Sep-2016  
Conference Location: Skukuza, South Africa  
**Paper Title:** Mid-Infrared detection in p-GaAs/AlGaAs heterostructures with a current blocking barrier  
**Authors:** A. G. U. Perera, Dilip Chauhan, Lianhe Li, Li Chen, Edmund Linfield  
Acknowledged Federal Support: **Y**

**Publication Type:** Conference Paper or Presentation **Publication Status:** 1-Published  
**Conference Name:** SPIE Microtechnologies  
Date Received: 08-Aug-2018 Conference Date: 08-May-2017 Date Published:  
Conference Location: Barcelona, Spain  
**Paper Title:** Infrared spectroscopy as a screening technique for colitis  
**Authors:** Jitto Titusa, Hemendra Ghimire, Emilie Viennoisb, Didier Merlin and A. G. Unil Perera  
Acknowledged Federal Support: **Y**

**DISSERTATIONS:**

**Publication Type:** Thesis or Dissertation  
**Institution:** Georgia State University  
Date Received: 25-Jul-2016 Completion Date: 7/29/16 5:38PM  
**Title:** Infrared Diagnostics on Micro and Nano Scale Structures  
**Authors:** Jitto Titus  
Acknowledged Federal Support: **Y**

**Publication Type:** Thesis or Dissertation  
**Institution:** Georgia State University  
Date Received: 20-Aug-2019 Completion Date: 1/5/19 1:17AM  
**Title:** MATERIAL AND TECHNIQUES FOR EXTENDED-WAVELENGTH AND SPLIT-OFF BAND INFRARED DETECTORS  
**Authors:** Dilip Chauhan  
Acknowledged Federal Support: **Y**

**Publication Type:** Thesis or Dissertation  
**Institution:** georgia State University  
Date Received: 31-Oct-2022 Completion Date: 5/11/21 6:50PM  
**Title:** Infrared Spectroscopy of Serum Samples for Disease Diagnostics  
**Authors:** Hemendra, Mani, Ghimire  
Acknowledged Federal Support: **Y**

**RPPR Final Report**  
as of 05-Dec-2022

**PATENTS:**

**Intellectual Property Type:** Patent Date Received: **20-Aug-2019**  
**Patent Title:** Tunable Hot Carrier Photodetector  
**Patent Abstract:** Various examples are provided for hot carrier spectral photo detectors that can be tuned. In on  
**Patent Number:** 10347783 B2  
Patent Country: USA  
Application Date: 27-Aug-2014 Application Status: 3  
Date Issued: 26-Feb-2016

**Intellectual Property Type:** Patent Date Received: **14-Jul-2020**  
**Patent Title:** Detection of Melanoma and Lymphoma by ATR-FTIR spectroscopy  
**Patent Abstract:**  
**Patent Number:** 16/545409  
Patent Country: USA  
Application Date: 20-Aug-2019 Application Status: 2  
Date Issued:

**Intellectual Property Type:** Patent Date Received: **31-Oct-2022**  
**Patent Title:** "Detection of Melanoma and Lymphoma by ATR-FTIR spectroscopy"  
**Patent Abstract:**  
**Patent Number:** US20200056991A1  
Patent Country: USA  
Application Date: 20-Aug-2019 Application Status: 3  
Date Issued: 20-Feb-2020

**Intellectual Property Type:** Patent Date Received: **31-Oct-2022**  
**Patent Title:** Tunable Hot Carrier Photodetector  
**Patent Abstract:**  
**Patent Number:** AU2014347256 B2  
Patent Country: AUS  
Application Date: 16-Feb-2016 Application Status: 3  
Date Issued: 06-Dec-2018

**Partners**

I certify that the information in the report is complete and accurate:

Signature: Unil Perera

Signature Date: 11/4/22 9:32AM

## Final Report Upload

### 1. Abstract

The research carried out during this period produced an exciting novel concept which can revolutionize the IR detector design. Our novel detector consists of a graded injector barrier using Al GaAs and a flat collector barrier separated by an absorber/emitter (GaAs) (denoted as absorber from now on) with a barrier energy offset between the two barriers leading to a reduced dark current infrared detector. Our observed and unexpected results, published in Nature Photonics [1], showed an effective response wavelength threshold up to 55  $\mu\text{m}$ , for a device with a standard threshold of 3.9  $\mu\text{m}$  and led us to further explore the reason for the extended threshold with a dark current limited by the longer wavelength during this period. We have demonstrated that the barrier offset is a requirement to get the threshold extension and that the gradient will determine the strength and the extent of the extension. This concept will lead to the development of detectors with reduced dark current compared to conventional detectors with a similar wavelength threshold.

### 2.1 Broder Impacts

US Army support had a significant impact on training young scientists/engineers by propagating knowledge and promoting wide interactions with other industrial (NRC-Canada, NRC-SOREQ) and university laboratories (Michigan, New Mexico, Australian National, Leeds, UGA and Georgia Tech). Our Alumni are spread among industry and academia in places such as Inficon Inc., EG&G Judson Infrared, GE Infrastructure Sensing, IBM, Reuters, SPD Laboratories, Japan, Archcom Technologies Inc, Jayawardanapura University, GSU, Georgia Tech, Shanghai Jiao Tong University, US Air Force, and others. A program based on NSF GK-12 Fellows was initiated at an elementary school. We have worked with K-12 students, educators, and undergraduates, exposing them to hands on cutting-edge scientific experiments through REU and RET programs. Four K-12 teachers (2 each from Griffin Middle and Campbell high school IB program) were introduced to physics research. Experiments teachers developed at GSU are being carried out by students in their classes. High achieving high school students were exposed to physics research during a one week “Advanced Physics” Summer Camp (<http://www.phy-astr.gsu.edu/funphysicsdays.html>). Several of those participants have joined prestigious colleges including Harvard, Duke, Yale, MIT, U. Chicago, GA. Tech, and Emory. Some of these participants are now pursuing Ph.Ds. (MIT, Berkley) and M.Ds. (Pitt, Emory, Case Western and Stanford). Students were also exposed to a surgeon treating epileptic seizures with E-M radiation, a sports physician connecting Newton’s laws to concussions, an F-16 engineer, a logistics company CEO, a virologist and the GSU Provost explains how physics is useful in their careers. The PI also worked with University of West Georgia (Dr. A. De Silva), Advanced Academy, where high achieving high school students are admitted into an accelerated undergraduate program.

### 3. Findings: Completed Work

#### 3.1 Significance of the Project

Dark current is an unavoidable fact, in any photoconductive detector. A common technique to decrease the dark current is to lower the operating temperature, making the detector operation costlier and cumbersome. Reducing dark current without cooling will be an advantage, especially for longer wavelength detectors. The threshold wavelength of conventional Infrared (IR) detectors is determined by the relation  $\lambda_t = 1.24/\Delta$  and the dark current will also depend on the  $\Delta$ . The proposed device with an effective  $\Delta'$  for photo detection ( $\Delta' \ll \Delta$ ) with a longer effective wavelength threshold ( $\lambda_{\text{eff}} = 1.24/\Delta'$ ) will have a dark current determined by the original  $\Delta$ . The advantage of this detector will be an extended effective threshold wavelength with a dark current advantage. Understanding this work will not only advance fundamental hot-carrier physics, but also advance detector technology by developing a novel detector operating beyond the spectral limit with a reduced dark current. Using this idea, existing semiconductor detectors (in any material system) can operate with a longer wavelength range detector with a dark current corresponding to the original threshold. This idea can be further employed to reduce the energy consumption of most of the electronic components leading to large scale savings, by reducing unwanted (as heat) energy usage.

### 3.2 Surface Plasmon Enhancements for Optimizing Detectors Performance

Our experimental [2] and theoretical [3] studies on metal corrugated surface plasmon structures show enhanced optical absorption. The main features of these spectra are: (i) Resonant absorption spanning the mid-infrared spectral window; (ii) Blue-shift of resonant-peak wavelength ( $\lambda_p$ ) with increasing metallic height (iii) Red-shift of  $\lambda_p$  with increasing grating period and (iv) Absorption enhancement of using plasmonic metal corrugation compared to the bare structure without the plasmonic structure. We have also shown experimentally the polarization sensitivity of quantum well infrared photodetectors (QWIPs) coupled to a diffraction grid [4] with 8.4  $\mu\text{m}$  response peak showing polarization sensitivity.

### 3.3 Effects of the graded barrier and barrier offset

The research performed in developing reduced dark current photodetectors include studying the dynamics of hot carriers in a structure with a graded injector barrier and a barrier energy offset. The dark current of the proposed detector is determined by an activation energy corresponding to a shorter wavelength ( $\lambda_t$ ) than the observed threshold wavelength ( $\lambda_{\text{eff}}$ ) of the device. In general, the standard expected threshold wavelength ( $\lambda_t$ ) of a photodetector is governed by the spectral rule  $\Delta = 1.24/\lambda_t$ , where  $\Delta$  is the standard activation energy (associated with growth and design) controlling the dark current. However, in the proposed detector (graded injector barrier with a barrier energy offset), the dark current depends upon  $\Delta$ , (as grown) while the effective response threshold wavelength ( $\lambda_{\text{eff}}$ ) is governed by a  $\Delta' = 1.24/\lambda_{\text{eff}}$ , with an effective activation energy  $\Delta' \ll \Delta$ . The  $\Delta'$  will be across the absorber and the collector barrier interface, while  $\Delta$  will still be the activation energy at the graded injector barrier and the absorber interface (see Fig. 1). A p-type GaAs absorber, sandwiched between a higher energy graded  $\text{Al}_x\text{Ga}_{1-x}\text{As}$  injector barrier corresponding to  $\Delta$  and lower energy constant  $\text{Al}_x\text{Ga}_{1-x}\text{As}$  collector barrier, provides the active region of the proposed device.

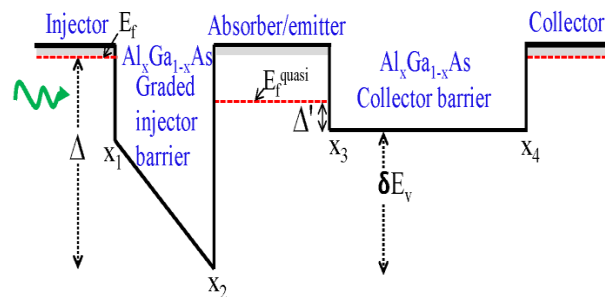


**Figure 1.** The unbiased valence band (VB) diagram of the detector with a graded injector barrier and barrier energy offset ( $\delta E_v$ ), where the injector, absorber/emitter (absorber) and collector are p doped GaAs. The mole fractions of Al in the  $\text{Al}_x\text{Ga}_{1-x}$ .

$x$ As graded injector and collector barriers are given by  $x_1$ ,  $x_2$  and  $x_3 = x_4$ .  $\Delta$  is the activation energy primarily determined by the Al mole fraction.  $\Delta'$  is effective activation energy at the absorber-collector barrier interface which gives rise to the  $\lambda_{\text{eff}}$ .

The energy difference between these two barriers is referred to as the barrier energy offset ( $\delta E_v$ ). Upon incident of infrared radiation, hot carriers are generated in the injector, absorber, and collector (for the transport process under appropriate bias, only the hot carrier from the injector is considered since the collector contribution is negligible). Due to  $\delta E_v$ , there is a sufficient amount of energy transfer from hot to cold carriers during hot-cold carrier interaction in the absorber and the carrier distribution function get significantly modified in the absorber. A quasi-Fermi energy distribution will be formed in the absorber at a carrier temperature ( $T_c$ ) which is greater than the lattice temperature ( $T_L$ ), which will be referred to as the hot carrier effect [34-36]. This hot-carrier effect which gives rise to a quasi-Fermi level ( $E_f^{\text{quasi}}$ ), provides the effective activation energy  $\Delta'$ , for photo detection, while the dark current will still be controlled by  $\Delta$  at the injector and absorber interface. Understanding the process of hot-cold carrier interaction and energy transfer in the absorber will be essential for designing high performance reduced dark current photodetectors. The value of  $\Delta'$  in proposed detectors depends on the number of hot carriers and the amount of energy exchange during the interaction with cold carriers in the absorber that consequently depends both on  $\delta E_v$  and the gradient of the injector barrier. Thus, by designing detectors with different  $\delta E_v$  values and gradients and obtaining the results (signal strength and  $\lambda_{\text{eff}}$ ) modeling exercises can be carried out. Therefore, the proposal includes studying the injection of hot carriers, hot-cold carrier interaction, and simulation of hot carrier dynamics to design, develop and optimize the detectors with the dark current advantage. The following steps will be carried out to achieve the proposal goals.

### 3.4. Conventional (symmetric) Photodetectors

The conventional (symmetric) heterojunction IR detector consists of p-doped GaAs absorber and undoped  $\text{Al}_x\text{Ga}_{1-x}\text{As}$  barrier layers. The VB diagram of the unbiased conventional detector is shown in Fig. 2 (see Table 2 for parameters for different detectors). The main mechanisms governing the operation of this photodetector are photon absorption generating hot carriers, interaction of hot carriers, and the collection of hot carriers [5, 6]. It is observed that due to the symmetry ( $\delta E_v = 0$ ) of the detector, exchange of energy during hot-cold carrier interaction does not provide sufficient modifications to the carrier distribution function in the absorber. Hence the Fermi level ( $E_f$ ) will not be changed (no effective  $\Delta'$ ). At zero electric field, no photo response is observed (in an ideal symmetric detector) which implies no net flow of hot holes. However, applying an electric field, a spectral response with threshold wavelength  $\lambda_t = 1.24/\Delta$  is observed.

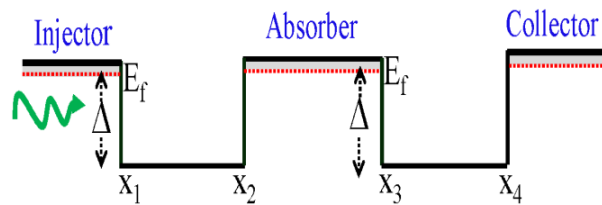


**Figure 2.** The unbiased VB diagram of conventional symmetric detector where the injector, absorber, and collector are p-doped GaAs with  $x_1 = x_2 = x_3 = x_4$  are the mole fractions of Al in the  $\text{Al}_x\text{Ga}_{1-x}\text{As}$  barriers,  $\Delta$  is the standard activation energy corresponds to spectral response threshold wavelength ( $\lambda_t = 1.24/\Delta$ ). See Table 2 for parameters for standard devices.

In general, the dark current of the photodetector is described by a 3D carrier drift model, shown below [5, 7]:

$$I_{dark} = 2Aev(F) \left( \frac{m^* k_B T}{2\pi\hbar^2} \right)^{3/2} \exp\left(-\frac{(\Delta - \alpha F)}{k_B T}\right) \quad (1)$$

Here, A is the electrically active area of the detector, e is the electronic charge,  $\Delta$  is the standard activation energy,  $v(F)$  is the carrier drift velocity as a function of electric field,  $m^*$  is the effective mass,  $k_B$  is Boltzmann's constant, T is temperature,  $\hbar$  is the reduced Planck's constant and  $\alpha$  is a fitting parameter that determines effective barrier lowering due to the applied field [5]. For a given value of the electric field, the  $I_{dark} \propto T^{3/2} \exp(-\Delta/kT)$  and  $\lambda_t = 1.24/\Delta$  [8, 9].

The experimental dark current of several conventional samples were fitted by the 3D drift model using Eq. 1 to confirm the validity of the model. The fitted dark currents (solid red lines) and the experimentally measured dark currents for HE0204 (■), SP1 (▲) and SP2 (★) with excellent agreements are shown in Fig. 3. The dark current data for LH1002 and the spectra for samples in Table 2 were published [1-3,29]. The detectors HE0204, SP1 and SP2, with  $\lambda_t = \lambda_{eff}$  of 16.1  $\mu\text{m}$ , 8.2  $\mu\text{m}$ , and 6.0  $\mu\text{m}$  respectively agree with the  $\Delta$  used for dark current model. A simulated dark current for a conventional modelled detector (labeled as M) of  $\Delta = 0.091$  eV (13.7  $\mu\text{m}$ ) is also shown by the dotted green (•••) line in Fig. 3.

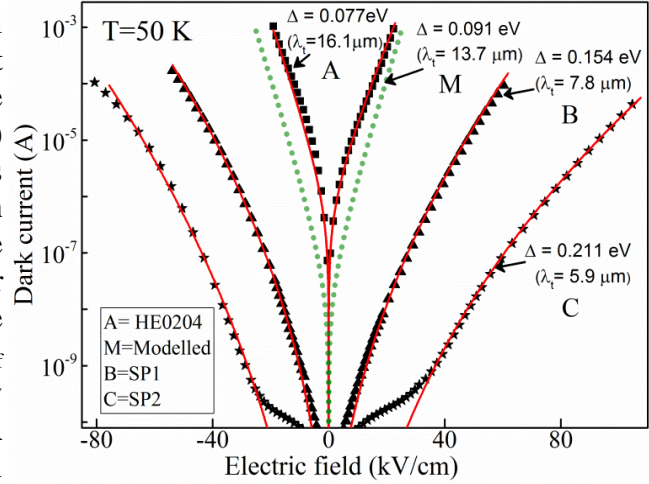


**Figure 3.** Experimental and 3D model dark current for the samples HE0204 (■), SP1 (▲) and SP2 (★). In addition, a simulated dark current for a modelled detector (•••) of 13.7  $\mu\text{m}$  using 3D drift model.

This modelled device has a reasonable dark current (lower than 16.1  $\mu\text{m}$  and higher than 7.8  $\mu\text{m}$ ) for a 13.7  $\mu\text{m}$  detector. These agreements clearly indicate the 3D carrier drift model for dark current is a reasonable model to obtain the dark current of detectors for a given  $\Delta$ .

**Table 2.** Device parameters for four conventional detector samples. p-doping, Al mole fraction, the standard activation energy  $\Delta$  associated with dark current (Eq.1) and corresponding threshold wavelength  $\lambda_t$ , effective activation energy  $\Delta'$  from the experimental spectral response  $\lambda_{eff}$  are also listed. For conventional devices  $\lambda_t \sim \lambda_{eff}$  (within the experimental uncertainties) indicating no hot carrier energy transfer. The thickness of the absorber in HE0204 is 120 nm, whereas for SP1, SP2, and LH1002 is 18.8 nm. The reported spectral response measured at 50 K and the threshold wavelength ( $\lambda_t$ ) of response for all samples were determined by temperature-dependent internal photoemission spectroscopy (TDIPS) fitting [10].

No.	Sample	p-doping (cm <sup>-3</sup> )	Al mole fraction x <sub>1</sub> = x <sub>2</sub> = x <sub>3</sub> =x <sub>4</sub>				$\Delta$ (eV)	$\lambda_t$ ( $\mu\text{m}$ )	$\Delta'$ (eV)	$\lambda_{\text{eff}}$ ( $\mu\text{m}$ )
A	HE0204	1×10 <sup>18</sup>	0.12	0.12	0.12	0.12	0.077	16.1	0.077	16.1
M	Modelled	1×10 <sup>19</sup>	0.22	0.22	0.22	0.22	0.091	13.7	0.091	13.7
B	SP1	3×10 <sup>18</sup>	0.28	0.28	0.28	0.28	0.154	7.8	0.144	8.2
C	SP2	3×10 <sup>18</sup>	0.37	0.37	0.37	0.37	0.211	5.9	0.190	6.0
D	LH1002	1×10 <sup>19</sup>	0.57	0.57	0.57	0.57	0.30	4.13	0.295	4.2

### 3.5 Dark Current Advantage with Effective Activation Energy ( $\Delta'$ )

Detectors with different barrier energy offsets and gradients (listed in Table 3) were grown and photo response spectra and dark currents were measured. Next, these samples were compared with conventional detectors with similar wavelength thresholds to show the effect of those parameters on the dark current advantage due to the effective activation energy ( $\Delta'$ ).

**Table 3.** Samples used to study the effect of the gradient and barrier energy offset. Device parameters and the corresponding standard activation energy ( $\Delta$ ), threshold wavelength ( $\lambda_t$ ), the effective activation energy ( $\Delta'$ ) and effective threshold wavelength ( $\lambda_{\text{eff}}$ ) at 50 K for the samples listed. The thickness of the absorber is 80 nm for all three samples. For SP1001, spectral photo response at 5.3 K also shown, since at 50 K,  $\lambda_{\text{eff}}$  close to  $\lambda_t$ .

Sample	p-doping (cm <sup>-3</sup> )	Al mole fraction				$\delta E_v$ (eV)	$\Delta$ (eV)	$\lambda_t$ ( $\mu\text{m}$ )	$\Delta'$ (eV)	$\lambda_{\text{eff}}$ ( $\mu\text{m}$ )
		x <sub>1</sub>	x <sub>2</sub>	x <sub>3</sub>	x <sub>4</sub>					
SP1001	1×10 <sup>19</sup>	0.75	0.75	0.57	0.57	0.10	0.40 0.40	3.1 3.1	0.302 0.034	4.1 at 50 K ~36 at 5.3 K
SP1007	1×10 <sup>19</sup>	0.45	0.75	0.57	0.57	0.10	0.40	3.1	0.139	8.9
15SP3	1×10 <sup>19</sup>	0.45	0.75	0.39	0.39	0.19	0.40	3.1	0.090	13.7

#### 3.5.1 Effect of the barrier energy offset (with flat injector barrier)

The unbiased VB diagram of a conventional detector (LH1002) and a flat injector barrier detector (SP1001) with a barrier energy offset ( $\delta E_v$ ) are shown in Fig. 4(a) and (b). As compared to conventional detectors (Table 2), although designed for 3.1  $\mu\text{m}$ , SP1001 shows a  $\lambda_{\text{eff}}$  of ~ 36  $\mu\text{m}$  (at 5.3 K) changing to 4.1  $\mu\text{m}$  at 50 K (Inset of Fig. 4 (c)). The  $\lambda_{\text{eff}}$  approach the  $\lambda_t$  as the temperature is increased (from 5.3 K to 50 K). However, this clearly indicates that the  $\delta E_v$  is critical to obtain the  $\Delta'$  which gives a  $\lambda_{\text{eff}}$  ( $\gg \lambda_t$ ) in a flat injector barrier detector with barrier energy offset whereas the dark current is still determined by  $\Delta$ . This also shows that  $\lambda_{\text{eff}}$  depends on the operating temperature, which could be due to the dependence of hot carrier lifetime or dependence of scattering (carrier-carrier) on the operating temperature which will be discussed later. Here, the  $\delta E_v$  is critical to obtain a  $\lambda_{\text{eff}}$ , (different from  $\lambda_t$ ) which gives the dark current advantage in studied detectors as compared to the conventional detectors.

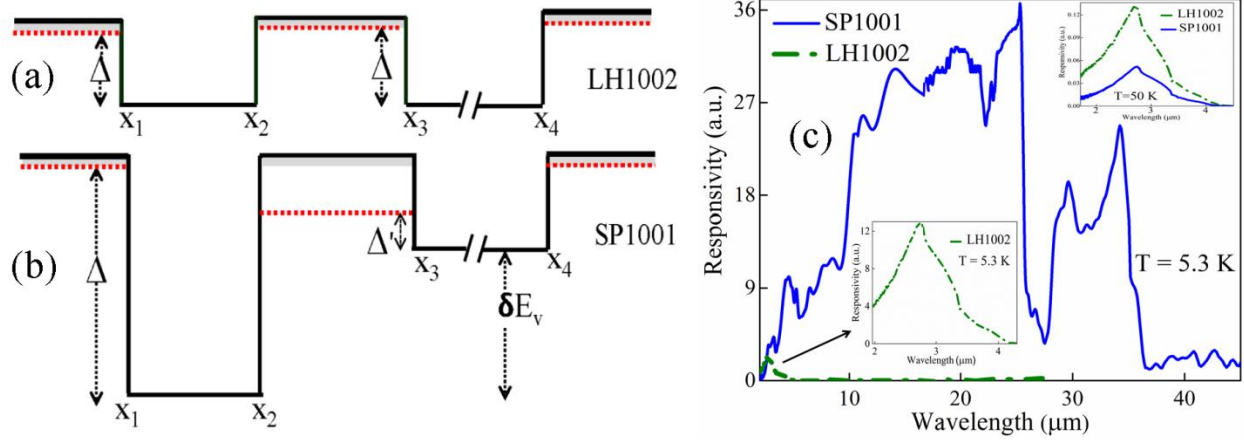


**Figure 4.** Unbiased VB diagram of (a) LH1002 (b) SP1001,  $\delta E_v = 0.10$  eV (c) The spectra of SP1001 at 5.3 K shows  $\lambda_{\text{eff}} \sim 36 \mu\text{m}$ , inset shows spectra of SP1001 and LH1002 at 50 K, which shows  $\lambda_{\text{eff}} = 4.1 \mu\text{m}$  for SP1001 which agrees with the conventional  $\lambda_t = \lambda_{\text{eff}} = 4.2 \mu\text{m}$  of LH1002.

### 3.5.2 Effect of the gradient of the injector barrier (with the same barrier energy offset)

The photo response of two devices with the same barrier energy offset ( $\delta E_v$ ) but with a graded (SP1007) and flat (SP1001) injector barriers are compared at 50 K (Fig. 5). Zero bias VB diagram is shown in the inset. At 50 K, for SP1007 a  $\lambda_{\text{eff}} = 8.9 \mu\text{m}$  ( $\Delta = 0.139$  eV) was observed, although for SP1001,  $\lambda_{\text{eff}} = 4.1 \mu\text{m}$  is closer to the  $\lambda_t$  (see the Table. 2). However, as the temperature is reduced, the  $\lambda_{\text{eff}}$  increases to  $\sim 36 \mu\text{m}$  at 5.3 K for SP1001 [see Fig. 4 (c)]. As the gradient of the injector barrier is increased (without changing the  $\delta E_v$ ), it is also shown that the  $\lambda_{\text{eff}}$  is increased. This implies that by adjusting the gradient of the injector barrier, the  $\lambda_{\text{eff}}$  can be increased leading to a better dark current advantage which will be discussed in section 3.5.

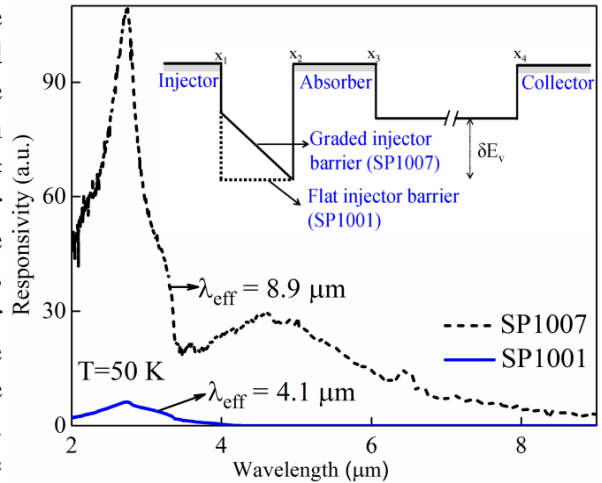


**Figure 5.** Response spectra of SP1001 and SP1007, as injector barrier changes from flat to graded, the  $\lambda_{\text{eff}}$  increases from  $4.1 \mu\text{m}$  to  $8.9 \mu\text{m}$ .

Hence it can be inferred that, although, the  $\delta E_v$  is critical, the gradient at the injector barrier is also important for controlling  $\lambda_{\text{eff}}$  at higher temperatures.

### 3.5.3 Effect of different barrier energy offsets (with the same gradient)

The photo response of two samples with similar graded injector barriers, but different barrier energy offsets are shown in Fig. 6. As  $\delta E_v$  increases (from 0.10 eV to 0.19 eV), the  $\lambda_{\text{eff}}$  increases (from  $8.9 \mu\text{m}$  to  $13.7 \mu\text{m}$ ). This suggests that by using a suitable value of  $\delta E_v$  (for a suitable graded injector barrier), the  $\lambda_{\text{eff}}$  can be adjusted while maintaining the reduced dark current associated with  $\Delta$ . Hence obtaining a better dark current advantage (through increased  $\lambda_{\text{eff}}$ ) can be obtained using an increased barrier energy offset. A set of samples with varying  $\delta E_v$  could be used for confirmation and optimization. Detector samples with different barrier energy offsets

and gradients should allow one to understand the energy transfer process from hot carrier to cold carrier leading to the dark current advantage.

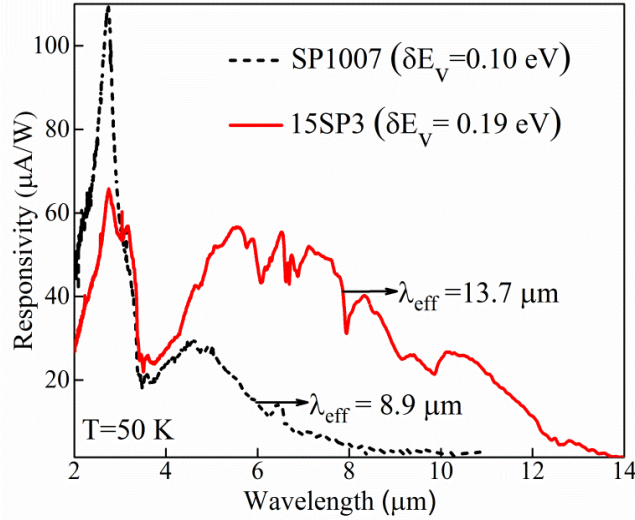


**Figure 6.** Photo response spectra of SP1007 and 15SP3. An increase in  $\lambda_{\text{eff}}$  from 8.9  $\mu\text{m}$  to 13.7  $\mu\text{m}$  is observed as  $\delta E_v$  increases from 0.10 eV to 0.19 eV.

### 3.6 Graded Injector with Barrier Energy Offset for Dark Current and $D^*$ Advantage

In section 3.4, we showed that the barrier energy offset ( $\delta E_v$ ) and the gradient of the injector barrier is important to observe an increased  $\lambda_{\text{eff}}$ . Here our focus is to demonstrate the dark current advantage. However, for the reduced dark current detector to provide an advantage, it should also have a specific detectivity ( $D^*$ ) that is comparable or better than for the conventional detector. Section 3.5.1 shows the dark current advantage with a detector with a  $\lambda_{\text{eff}}$ . Section 3.5.2 shows the dark current advantage, simultaneously with a  $D^*$  advantage.

Two sets of samples consisting of a conventional detector and a graded injector barrier with barrier energy offsets were studied with similar structure parameters except for the differences in the  $\delta E_v$ . A conventional detector SP1 (with  $\delta E_v = 0$  and no gradient) gives a  $\lambda_t (= \lambda_{\text{eff}})$  of 8.2  $\mu\text{m}$  and SP1007 ( $\delta E_v = 0.10$  eV and a graded injector barrier) has a  $\lambda_t$  expected around 3.1  $\mu\text{m}$ , but shows  $\lambda_{\text{eff}}$  up to 8.9  $\mu\text{m}$  at 50 K. Similarly, another conventional detector HE0204 ( $\delta E_v = 0$  and no graded injector barrier) is designed to give a  $\lambda_t = 16.1$   $\mu\text{m}$  and 15SP3 ( $\delta E_v = 0.19$  eV and graded injector barrier) has a  $\lambda_t$  expected around 3.1  $\mu\text{m}$ , but shows  $\lambda_{\text{eff}}$  of 13.7  $\mu\text{m}$  at 50 K.

#### 3.6.1 Dark current advantage with a graded injector barrier and barrier energy offset

The experimental ( $\blacksquare, \blacktriangle$ ) and 3D model dark current (solid red lines) with an experimental photo response for SP1 and SP1007 at 50 K are shown in Fig. 7 (a) and (b). The  $\Delta$  values used for the dark current fitting for SP1 give a  $\Delta = 0.154$  eV, i.e.  $\lambda_t = 7.8$   $\mu\text{m}$  while SP1007 gives  $\Delta = 0.40$  eV corresponding to  $\lambda_t = 3.1$   $\mu\text{m}$ . A value for  $\lambda_{\text{eff}} = 8.2$   $\mu\text{m}$  was observed for the standard detector SP1 which corresponds to  $\Delta' = 0.151$  eV, closely matching the dark current fitting value  $\Delta = 0.154$  eV. However, for SP1007, the  $\lambda_{\text{eff}} = 8.9$   $\mu\text{m}$  corresponds to  $\Delta' = 0.139$  eV, which is much lower than the  $\Delta = 0.40$  eV ( $\lambda_t = 3.1$   $\mu\text{m}$ ) used for the dark current fitting. Hence, the SP1007 while showing an effective threshold of  $\lambda_{\text{eff}} = 8.9$   $\mu\text{m}$ , the dark current matches a conventional detector with a  $\lambda_t = 3.1$   $\mu\text{m}$  ( $\Delta = 0.40$  eV) threshold. Fig. 7 (b) shows that both the peak and FWHM responsivity for SP1007 is lower compared to SP1. The  $D^*$  of SP1007 (peak as well as in the FWHM range) is also lower than the conventional detector SP1. This can be overcome by increasing the  $\delta E_v$  as shown in the next section. The resulting increase in  $D^*$  will be critical for detectors with a dark current advantage.

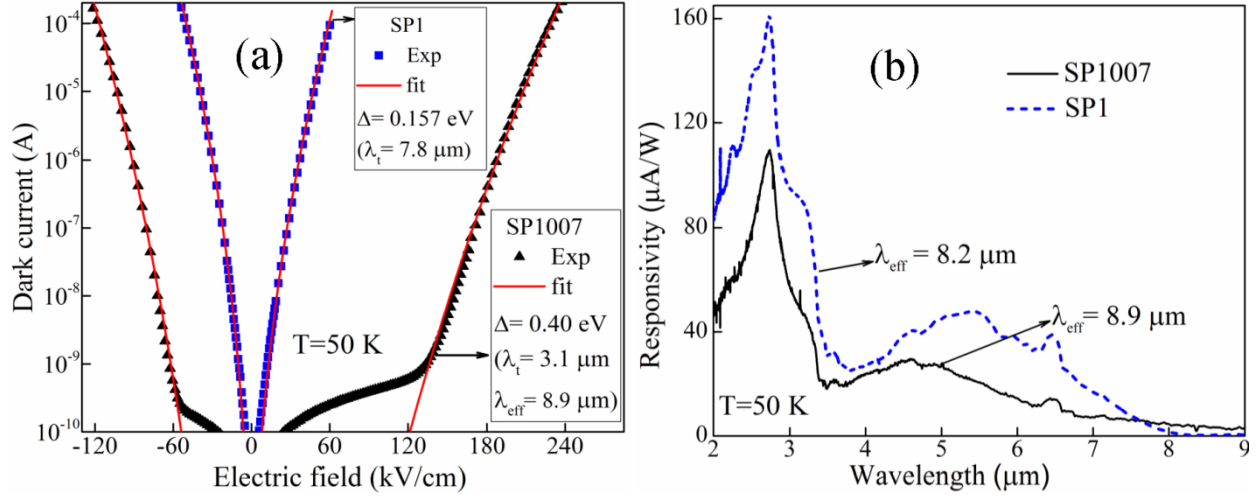


**Figure 7. (a)** Drift model (solid red line) and experimental dark current for SP1 (■) and SP1007 (▲), showing a clear difference in dark currents between the two structures **(b)** Response spectra of SP1007 shows  $\lambda_{\text{eff}} = 8.9 \mu\text{m}$  ( $\Delta' = 0.139 \text{ eV}$ )  $< \Delta = 0.40 \text{ eV}$  ( $\lambda_t = 3.1 \mu\text{m}$ ) obtained from dark current, whereas for SP1,  $\lambda_{\text{eff}} = 8.2 \mu\text{m}$  ( $\Delta' = 0.151 \text{ eV}$ ) matches with  $\Delta = 0.154 \text{ eV}$  obtained from dark current fitting.

### 3.6.2 Both dark current and $D^*$ advantages (increased barrier energy offset)

To achieve both the dark current and  $D^*$  advantages, 15SP3 ( $\delta E_v$  increased to 0.19 eV) and a conventional (HE0204) detector are shown in Fig. 8 (a) and (b). Dark current fit for a conventional model detector of  $\Delta = 0.091 \text{ eV}$  ( $\lambda_t = 13.7 \mu\text{m}$ ) is also shown by green dotted (••) line in Fig.8 (a).

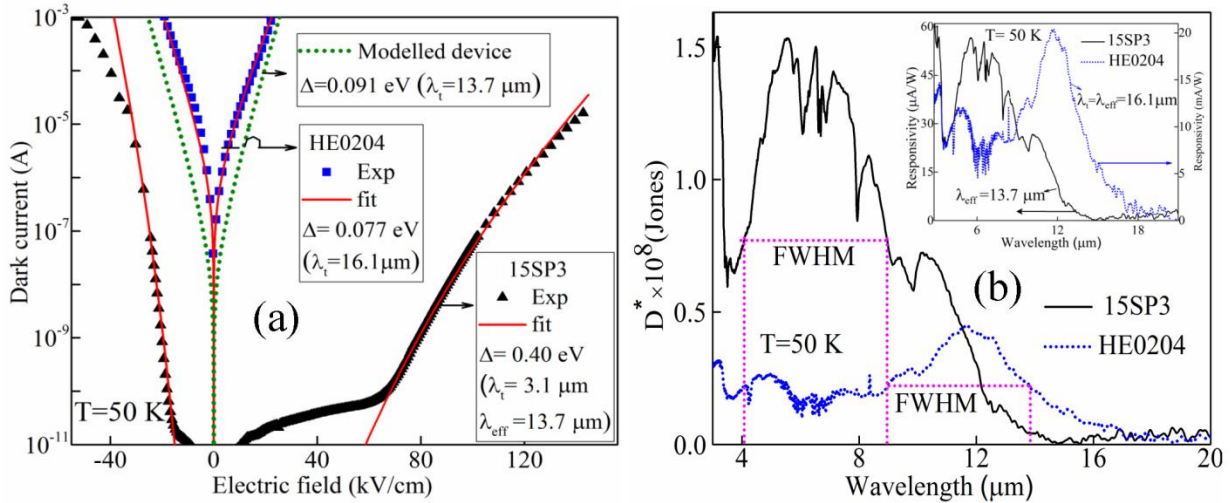


**Figure 8. (a)** Comparison of dark current for HE0204 (■) and 15SP3 (▲), a clear difference showing in dark current for both structures for similar  $\lambda_t$ . A dotted green (••) line shows a simulated dark current of a modelled detector with  $\Delta = 0.091 \text{ eV}$  ( $\lambda_t = 13.7 \mu\text{m}$ ). **(b)**  $D^*$  for HE0204 and 15SP3, clearly showing a higher  $D^*$  for 15SP3, Inset shows response of HE0204,  $\lambda_{\text{eff}} = 16.1 \mu\text{m}$  ( $\Delta' = 0.077 \text{ eV}$ ) which was fitted to dark current with  $\Delta = 0.077 \text{ eV}$ ; for 15SP3,  $\Delta'$  ( $\lambda_{\text{eff}}$ ) is 0.091 eV ( $13.7 \mu\text{m}$ ) fitted to dark current with  $\Delta = 0.40 \text{ eV}$  corresponding to  $\lambda_t = 3.1 \mu\text{m}$ .

The  $\Delta$  values used for dark current fittings for HE0204 is  $\Delta = 0.077 \text{ eV}$ , i.e.  $\lambda_t = 16.1 \mu\text{m}$  (matches experimental threshold) and for 15SP3,  $\Delta \sim 0.40 \text{ eV}$  i.e.  $\lambda_t = 3.1 \mu\text{m}$  which shows an

experimental  $\lambda_{\text{eff}}$  of 13.7  $\mu\text{m}$  ( $\Delta = 0.091$  eV) (Fig. 8 (a) and (b)). Since the existing conventional device has a  $\lambda_t = 16.1$   $\mu\text{m}$  (HE0204), a modelled device (listed M in Table 2) with a  $\lambda_t$  of 13.7  $\mu\text{m}$  is used for justifying the dark current advantage. The dark current of 15SP3 is also much lower than both the  $\lambda_t = 16.1$   $\mu\text{m}$  threshold device and the simulated dark current of the modelled device with  $\lambda_t = 13.7$   $\mu\text{m}$ . This again confirms the dark current advantage as compared to conventional detector. The specific detectivity ( $D^*$ ) for both samples are shown in the Fig. 8 (b), where the  $D^*$  (both peak and FWHM) is higher in 15SP3 as compared to the conventional device HE0204 (see Table 4). Inset of Fig. 8 (b) shows that responsivities of HE0204 and 15SP3, although the responsivity for the conventional device (HE0204) is higher, due to the dark current advantage, the  $D^*$  is higher with  $\lambda_{\text{eff}} = 13.7$   $\mu\text{m}$  for 15SP3.

This confirms the proposed idea of longer threshold wavelength detector with a reduced dark current and  $D^*$  advantage in graded injector barrier with barrier energy offset detector as compared to a conventional detector. However, further understanding is needed for designing specific detectors. During this project, a series of samples with different values of barrier energy offset and graded injector barriers will be grown and characterized.

**Table 4.** The value of FWHM responsivity and FWHM  $D^*$  for HE0204 and 15SP3 at  $T = 50$  K.

Sample	FWHM		
	Wavelength Range ( $\mu\text{m}$ )	$D^*$ (Jones)	Responsivity (A/W)
15SP3	4.0-8.9	$7.6 \times 10^7$	$28.3 \times 10^{-6}$
HE0204	8.9-13.8	$2.2 \times 10^7$	$10.1 \times 10^{-3}$

### 3.7 The Effect of Temperature on the Effective Activation Energy ( $\Delta'$ )

The temperature dependent photo response of 15SP3 from 50 to 100 K (inset shows 5.3 K) is shown in Fig. 9 (a). A decrease in  $\lambda_{\text{eff}}$  from 45  $\mu\text{m}$  to 3.1  $\mu\text{m}$  is observed as the temperature is increased from 5.3 K to 100 K. A possibility for the change in effective  $\Delta'$  can be the decreased lifetime of the hot carriers with increasing temperature, making the energy transfer process less efficient [11]. In addition, carrier-carrier energy transfer can be less efficient by processes, such as carrier-ionized dopant scattering, causing a reduced carrier-carrier scattering rate [12, 13].

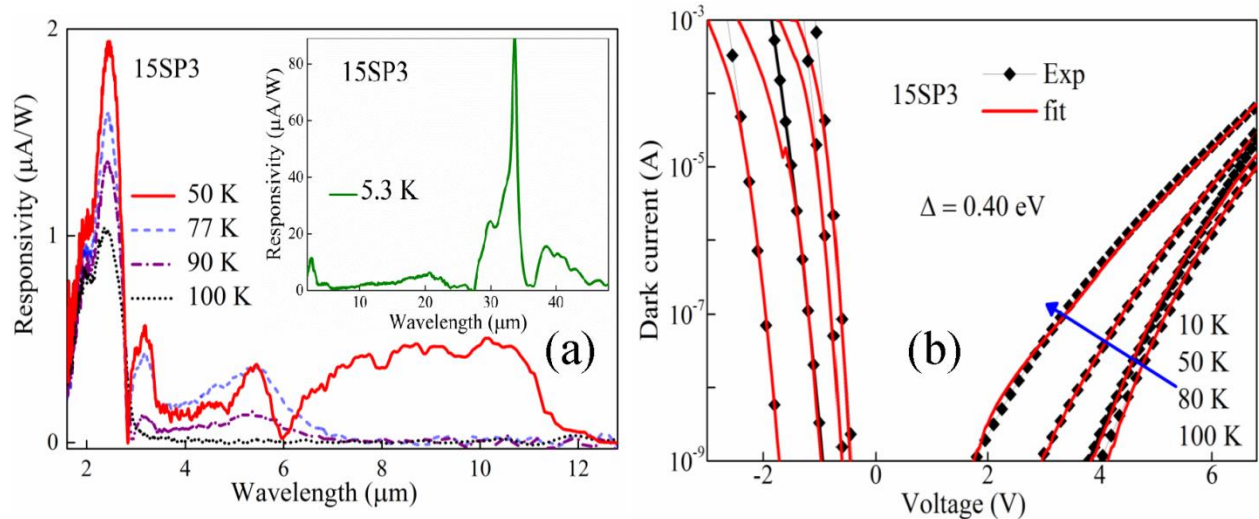


**Figure 9. (a)** Effect of temperature on the  $\lambda_{\text{eff}}$  of 15SP3 from 50 K to 100 K: Inset shows the response at 5.3 K; the  $\lambda_{\text{eff}}$  changes from 45  $\mu\text{m}$  to 3.1  $\mu\text{m}$  as the temperature changes from 5.3 K to 100 K **(b)** Experimentally measured and fitted dark current curves in the temperature range 10 K –100 K for 15SP3.

In this regard, carrier lifetimes of 53, 35, and 14 nanoseconds respectively, at 40 K, 60 K, and 80 K, for a DWELL infrared detector [40], indicate the effective Fermi energy shift will be reduced as the temperature is increased due to the reduced lifetime of hot carriers. The temperature dependent dark current (10 K-100 K) and their fitted curves using Eq. (1), agrees well with the designed value of  $\Delta = 0.40$  eV as shown in Fig. 9(b). From the dark current fitting curves,  $\Delta = 0.40$  eV remains constant at each temperature. However, the photo response threshold energy varies with temperature ( $\Delta' = 0.027$  eV to 0.40 eV) as shown in Fig. 9(a).

This also confirms that the dark current is determined by design  $\Delta$  while the effective threshold energy  $\Delta'$  ( $\Delta' \ll \Delta$ ) varies with temperature further confirming the dark current advantage in the proposed design as compared to conventional detectors. Further investigations will be carried out to understand the dependence of  $\Delta'$  ( $\lambda_{\text{eff}}$ ) on operating temperature.

### 3.8 A Basic Empirical Model for Hot Carrier Effects in the Extended Thershold Detectors

The dark current advantage described in connection with  $\lambda_{\text{eff}}$  ( $\Delta'$ ) in proposed detectors can be explained based on the hot - cold carrier interaction in the absorber [31, 32, 33]. The VB diagram of the proposed device is shown in Fig. 10 (a),  $E_f$  is the Fermi level at a lattice temperature ( $T_L$ ) and  $E_f^{\text{quasi}}$  is the quasi Fermi level at a hot carrier temperature ( $T_c$ ) (The absorber section is separated in Fig. 10 (b) for clarity). With incident of IR photons, hot holes with energy  $>\Delta$  will surmount the injector graded barrier and interact with cold holes in the absorber (contribution from the collector side is ignored in this discussion). In Fig. 10 (a) and (b), the solid (●) dots and an empty (○) dots represent hot hole and cold hole in the absorber, the green wavy arrow represents an incident photon with an energy exceeding  $\Delta$ , whilst the red wavy arrow in the absorber shows an incident photon with an energy  $\Delta'$ .

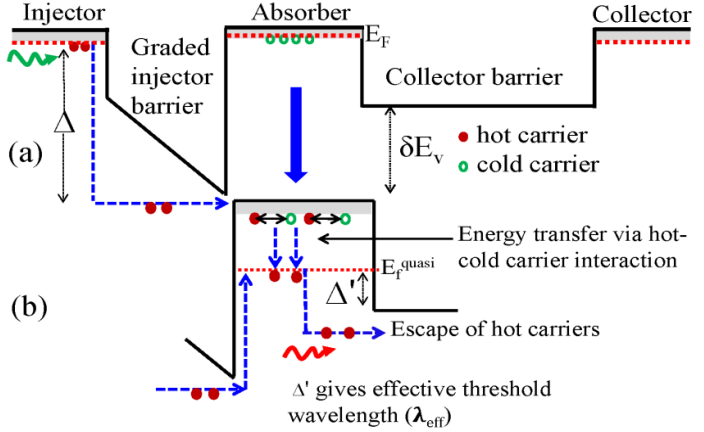
At zero bias, a net flow of hot carriers from graded injector to collector barrier will be observed owing to the difference in barrier heights. For a net flow of hot carriers  $\delta E_v$  is critical and increasing  $\delta E_v$  and the gradient of the injector barrier, will increase the flow. Some fraction of hot hole energy is transferred to the cold hole (in absorber), leading to non-equilibrium carrier densities with specific momentum states and elevated carrier temperature. As the system evolves towards equilibrium via momentum and energy relaxation, on a femtosecond or pico second time scale via elastic and inelastic scattering [14, 15]. All optical phonons generated eventually decay via multi phonon processes and this decay time depends on the lattice temperature, which varies from 10 ps at cryogenic temperatures to 4 ps or less at room temperature for thin films [16, 17]. On the same time scale, carrier-carrier scattering results in coulomb thermalization and allows the carrier system to be described by a quasi-Fermi Dirac distribution with temperature  $T_c \gg T_L$ . As a long wavelength ( $\lambda_{\text{eff}}$ ) photon with energy greater than ( $\Delta'$ ) is absorbed at this quasi- Fermi level ( $E_f^{\text{quasi}}$ ) hot holes will escape and collected across the collector barrier. Similar to the case in a conventional detector, with increasing bias, (up to a certain limit) the energy of holes passing over the graded barrier increases, leading to a greater transfer of energy to the cold holes in the absorber and in turn increases the number of hot holes in the absorber. Hence the number of hot holes escaping from the  $E_f^{\text{quasi}}$  over the collector barrier also increases, thereby increasing the response strength of the extended wavelength photo response.

To calculate the escape probability of hot carriers, escape cone model with  $E_f^{\text{quasi}}$  will be used. The responsivity (R) of the detector depends on the total quantum efficiency ( $\eta$ ), electron charge (q), speed of light in vacuum (c) and Planck's constant (h) as given by [5, 18, 19]

$$R = q\eta\lambda/hc$$

(2) [ENREF 25](#)

**Figure. 10. (a)** Unbiased schematic VB diagram of graded injector barrier with barrier energy offset.  $E_f$  is Fermi level at a lattice temperature ( $T_L$ ), upon photoexcitation hot holes surmount the graded injector barrier and interact with cold holes in the absorber. For clarity, the absorber section is separated. **(b)** Energy transfer via hot-cold hole interaction and the formation of quasi Fermi level ( $E_f^{quasi}$ ) at a hot hole temperature greater than the lattice temperature and finally the escape of hot holes from that  $E_f^{quasi}$  by absorption of long wavelength photon giving  $\Delta'$ .



[ENREF 25](#)

The total quantum efficiency ( $\eta$ ) is the product of the photon absorption probability ( $\eta_a$ ), the internal quantum efficiency ( $\eta_i$ ), and the hot carrier transport probability ( $\eta_t$ ) and is given as:

$$\eta = \eta_a \eta_i \eta_t \quad (3)$$

The value of  $\eta_a$  and  $\eta_t$  were calculated using the model described elsewhere [5, 19].  $\eta_i$  was calculated using an escape cone model [6] and calculation of  $\eta_i$  can take into account scattering of hot holes with cold holes as well as phonons, given by [6]:

$$\eta_i = \eta_0 + \left[1 - \frac{\eta_0}{\eta_M}\right] \gamma \eta_1 + \left[1 - \frac{\eta_0}{\eta_M}\right] \left[1 - \frac{\eta_1}{\eta_M}\right] \gamma^2 \eta_1 + \dots \quad (4)$$

where  $\eta_n = \eta_0(E - nh\nu)$  and  $\gamma = L_h / (L_e + L_h)$ , here,  $n$  is the number of scattering events,  $\eta_M$  is the maximum quantum efficiency, and the value of  $\eta_0$  is defined as the fraction of hot holes captured prior to any bulk scattering events, and is given by,

$$\eta_0 = \frac{L^*}{W} \left(1 - e^{-W/L^*}\right)^{1/2} \cdot \eta_{Ideal} \quad (5)$$

where  $W$  is the width of the absorber, and  $\eta_{Ideal}$  is the ideal quantum efficiency.  $L^* = L_h \times L_p / (L_h + L_p)$  is the reduced scattering length of hot hole-cold holes,  $L_h$  is the hole-hole scattering length for hot-cold holes and  $L_p$  represents elastic scattering of hot holes with phonons and impurities, and multiple reflections of the excited hot holes from the surfaces of the absorber. The value of  $E_f^{quasi}$  can be determined by difference between valance band edge ( $\Delta E_v$ ) [10] and  $\Delta'$  as determined by TDIPS fitting of photo response spectra.

**Special Note:** Due to the COVID-19 pandemic University was closed for more than a year with all the research labs deemed not urgently needed being closed for personnel. Our grant was on no cost extension for most of the last 2 years where standard personnel expenses were charged to the grant (per University and Government agreements).

During the grant period, our group published 3 review articles and more than 20 refereed journal articles. We were also granted six patents during the same period.

---

**References**

- [1] Y.-F. Lao, A. G. U. Perera, L. H. Li, S. P. Khanna, E. H. Linfield, and H. C. Liu, "Tunable hot-carrier photodetection beyond the bandgap spectral limit," *Nat Photon*, vol. 8, pp. 412-418, 05//print 2014.
- [2] M. S. Shishodia, P. V. V. Jayaweera, S. G. Matsik, A. G. U. Perera, H. C. Liu, and M. Buchanan, "Surface plasmon enhanced IR absorption: Design and experiment," *Photonics and Nanostructures - Fundamentals and Applications*, vol. 9, pp. 95-100, 2// 2011.
- [3] M. S. Shishodia and A. G. U. Perera, "Heterojunction plasmonic midinfrared detectors," *Journal of Applied Physics*, vol. 109, pp. 043108-043108-9, 2011.
- [4] V. Apalkov, G. Ariyawansa, A. G. U. Perera, M. Buchanan, Z. R. Wasilewski, and H. C. Liu, "Polarization Sensitivity of Quantum Well Infrared Photodetector Coupled to a Metallic Diffraction Grid," *IEEE Journal of Quantum Electronics*, vol. 46, pp. 877-883, 2010.
- [5] D. G. Esaev, M. B. M. Rinzan, S. G. Matsik, and A. G. U. Perera, "Design and optimization of GaAs/AlGaAs heterojunction infrared detectors," *Journal of Applied Physics*, vol. 96, pp. 4588-4597, 2004.
- [6] M. B. Rinzan, S. Matsik, and A. G. U. Perera, "Quantum mechanical effects in internal photoemission THz detectors," *Infrared Physics & Technology*, vol. 50, pp. 199-205, 4// 2007.
- [7] D. Chauhan, A. G. U. Perera, L. H. Li, L. Chen, and E. H. Linfield, "Dark current and photoresponse characteristics of extended wavelength infrared photodetectors," *Journal of Applied Physics*, vol. 122, p. 024501, 2017.
- [8] M. B. M. Rinzan, A. G. U. Perera, S. G. Matsik, H. C. Liu, Z. R. Wasilewski, and M. Buchanan, "AlGaAs emitter/GaAs barrier terahertz detector with a 2.3 THz threshold," *Applied Physics Letters*, vol. 86, p. 071112, 2005.
- [9] A. G. U. Perera, H. X. Yuan, S. K. Gamage, W. Z. Shen, M. H. Francombe, H. C. Liu, M. Buchanan, and W. J. Schaff, "GaAs multilayer p+-i homojunction far-infrared detectors," *Journal of Applied Physics*, vol. 81, pp. 3316-3319, 1997.
- [10] Y.-F. Lao and A. G. U. Perera, "Temperature-dependent internal photoemission probe for band parameters," *Physical Review B*, vol. 86, p. 195315, 11/26/ 2012.
- [11] M. R. Matthews, R. J. Steed, M. D. Frogley, C. C. Phillips, R. S. Attaluri, and S. Krishna, "Transient photoconductivity measurements of carrier lifetimes in an InAs/In<sub>0.15</sub>Ga<sub>0.85</sub>As dots-in-a-well detector," *Applied Physics Letters*, vol. 90, p. 103519, 2007.
- [12] J. Shah, A. Pinczuk, A. C. Gossard, and W. Wiegmann, "Energy-Loss Rates for Hot Electrons and Holes in GaAs Quantum Wells," *Physical Review Letters*, vol. 54, pp. 2045-2048, 05/06/ 1985.
- [13] L. Rota and D. K. Ferry, "A theoretical investigation of carrier-carrier effects in ultrafast experiments," *Semiconductor Science and Technology*, vol. 9, p. 468, 1994.
- [14] D. J. Erskine, A. J. Taylor, and C. L. Tang, "Femtosecond studies of intraband relaxation in GaAs, AlGaAs, and GaAs/AlGaAs multiple quantum well structures," *Applied Physics Letters*, vol. 45, pp. 54-56, 1984.
- [15] S. Katayama, "Theory of energy relaxation of 2D hot carriers in GaAs quantum wells," *Surface Science Letters*, vol. 170, p. A249, 1986/04/03 1986.

- [16] A. Othonos, "Probing ultrafast carrier and phonon dynamics in semiconductors," *Journal of Applied Physics*, vol. 83, pp. 1789-1830, 1998.
- [17] A. Othonos, H. M. van Driel, J. F. Young, and P. J. Kelly, "Correlation of hot-phonon and hot-carrier kinetics in Ge on a picosecond time scale," *Physical Review B*, vol. 43, pp. 6682-6690, 03/15/ 1991.
- [18] S. G. Matsik, P. V. V. Jayaweera, A. G. U. Perera, K. K. Choi, and P. Wijewarnasuriya, "Device modeling for split-off band detectors," *Journal of Applied Physics*, vol. 106, p. 064503, 2009.
- [19] A. G. U. Perera, H. X. Yuan, and M. H. Francombe, "Homojunction internal photoemission far-infrared detectors: Photoresponse performance analysis," *Journal of Applied Physics*, vol. 77, pp. 915-924, 1995.